Dual-component structural plasticity mediated by αCaMKII-autophosphorylation on basal dendrites of cortical layer 2/3 neurones

by

Gillian Seaton, Gladys Hodges, Annelies de Haan, Aneesha Grewal,

Anurag Pandey, Haruo Kasai* and Kevin Fox

School of Biosciences, Cardiff University, Cardiff CF10 3AX, UK

*Graduate School of Medicine, University of Tokyo, Tokyo 113-0033, Japan

Running title: Dual Component structural plasticity in vivo

Pages: 33

Figures: 11

Tables: 2

Word count

Total:	13,468
Introduction:	648
Discussion:	1,472

Address for correspondence: Prof. Kevin Fox, School of Biosciences, Museum Avenue, Cardiff University, Cardiff CF10 3AX, UK foxkd@cardiff.ac.uk

Conflict of Interest statement. The authors declare that they have no conflict of interest regarding the research reported in this manuscript.

Acknowledgements: We should like to express our thanks to Sam Barnes for critical reading of the manuscript. We are also most grateful to the MRC (MR/N003896/1) for funding for this project and for both the MRC (MR/M501670/1) and AMED (Strategic international research cooperative program) for joint funding between the Fox and Kasai labs.

Abstract

Sensory cortex exhibits receptive field plasticity throughout life in response to changes in sensory experience and offers the experimental possibility of aligning functional changes in receptive field properties with underpinning structural changes in synapses. We looked at the effects of two different patterns of whisker deprivation in male and female mice; 'Chessboard deprivation', which causes functional plasticity and 'All deprived', which does not. Using 2-photon microscopy and chronic imaging through a cranial window over the barrel cortex, we found that layer 2/3 neurones exhibit robust structural plasticity, but only in response to whisker deprivation patterns that cause functional plasticity. Chessboard pattern deprivation caused dual-component plasticity in layer 2/3 by (1) increasing production of new spines that subsequently persisted for weeks and (2) enlarging spines-head sizes in the pre-existing stable spine population. Structural plasticity occurred on basal dendrites but not apical dendrites. Both components of plasticity were absent in αCaMKII-T286A mutants that lack LTP and experience-dependent potentiation in barrel cortex, implying that αCaMKII auto-phosphorylation is not only important for stabilisation and enlargement of spines but also for new spine production. These studies therefore reveal the relationship between spared whisker potentiation in layer 2/3 neurones and the form and mechanisms of structural plasticity processes that underly them.

Significance Statement

This study provides a missing link in a chain of reasoning that connects LTP to experience-dependent functional plasticity *in vivo*. We found that increases in dendritic spine formation and spine enlargement (both of which are characteristic of LTP) only occurred in barrel cortex during sensory deprivation that produced potentiation of sensory responses. Furthermore, the dendritic spine plasticity did not occur during sensory deprivation in mice lacking LTP and experience-dependent potentiation (αCaMKII auto-phosphorylation mutants). We also found that the dual-component dendritic spine plasticity only occurred on basal dendrites and not on apical dendrites, thereby resolving a paradox in the literature suggesting that layer 2/3 neurones lack structural plasticity in response to sensory deprivation.

Introduction

Understanding the relationship between functional and structural plasticity requires knowing where in the brain the functional plasticity takes place and then looking for the structural plasticity in that location. This issue is important for understanding processes underlying learning and memory. However, it is usually not possible to know where to look in the brain when plasticity is induced during learning because memories are distributed across networks of neurones within single brain structures and even relatively simple learned behaviours involve multiple brain regions, any of which could house the sought after structural changes (Hoffman and McNaughton, 2002; Josselyn and Frankland, 2018). From this view-point, understanding plasticity's structure-function relationship is more tractable when studied in sensory cortex and when induced by sensory deprivation because, in this case, the location of the functional plasticity is often well characterised.

Sensory deprivation causes functional plasticity in layer 2/3 in visual and somatosensory cortex (Fox and Wong, 2005). Layer 2/3 neurones increase their responses to sensory inputs spared from the deprivation and decrease their responses to sensory inputs that are deprived. Following whisker trimming in a chessboard pattern, layer 2/3 neurones increase their responses to spared whisker stimulation and decrease their responses to deprived whisker stimulation (Wallace and Fox, 1999b). These changes are known to be cortical rather than subcortical and to depend on cortical activity (Fox, 1994; Wallace et al., 2001). Potentiation of the spared whisker response depends on auto-phosphorylation of CaMKII (Hardingham et al., 2003), which is a key step in induction of LTP (Giese et al., 1998; Chang et al., 2017). Depression of the deprived response is known to depend on GluA1 and to occlude LTD (Hardingham et al., 2008; Wright et al., 2008). These findings and others have implicated Hebbian processes in experience dependent cortical plasticity (Glazewski and Fox, 1996; Glazewski et al., 2000; Wallace et al., 2001; Dachtler et al., 2011).

Although a great deal of work has been conducted on functional plasticity in layer 2/3 cells, to date most studies on spine dynamics and structural plasticity in the cerebral cortex have been carried out on layer 5 apical dendrites (Lendvai et al., 2000; Holtmaat et al., 2006; Wilbrecht et al., 2010; Keck et al., 2013). This can partly be explained by the availability of Thy-1 GFP lines, where the fluorophore is very conveniently expressed sparsely in a subset of layer 5 neurones and partly by the relative ease of imaging apical dendrites that lie close to the surface of the brain. However, functional plasticity in cortical layer 5 cells is complicated by the differences in plasticity mechanisms present in regular spiking (RS) and intrinsic bursting (IB) cells, whereas layer 2/3 neurones appear more uniform in mechanism (Jacob et al., 2012; Greenhill et al., 2015). Furthermore, it is not clear how structural plasticity of apical dendritic spines might be related to

functional changes in receptive fields, when most of the sensory input via thalamic and layer 4 projections to layer 5 neurones impinge on the basal not the apical dendrites (Petreanu et al., 2009). Even in layer 2/3 neurones, the basal dendrites tend to receive strong sensory input from VPm and layer 4 while apical dendrites receive the input from motor cortex (Petreanu et al., 2009; Hooks et al., 2011). In this study, we have focused on structural plasticity in layer 2/3 rather than layer 5 and on basal dendrites more than apical in an effort to rebalance these mismatches.

To understand structural changes related to potentiation mechanisms, we also compared the effect of whisker deprivation on plasticity in wild-types with that in CaMKII auto-phosphorylation mutants that lack cortical and hippocampal LTP (Giese et al., 1998; Hardingham et al., 2003). Our findings elucidate the relationship between structural and functional plasticity in the cortex and demonstrate a pivotal role for CaMKII in both functional and structural plasticity.

Methods

Animals and rAAV constructs

We used Male and female αCaMKII-T286A homozygous mutant mice, which have an Alanine substituted at the Threonine 286 location (Giese et al., 1998), and their wild-type litter-mates for imaging experiments (see Table 1). Animals were social-group housed with *ad libitum* food and water in a 12:12 hour normal light/dark cycle. All animal care and use was performed in compliance with the UK Animals (Scientific Procedures) Act 1986. The rAAVs were purchased from the University of Pennsylvania Vector Core:
rAAV2/1.CAG.FLEX.EGFP.WPRE.bGH (Allen Institute 854) and rAAV.CaMKII 0.4.Cre.SV40 (Allen Institute).

Trans-cranial window implantation and rAAV intracranial virus injection

Cranial windows were implanted using methods similar to those published previously (Chen et al., 2000; Mostany and Portera-Cailliau, 2008; Holtmaat et al., 2009). Briefly, mice were injected with dexamethasone (2 mg g−1 body weight), deeply anesthetized with isoflurane and head-fixed on an ultra-precise stereotaxic frame (Kopf model 963). After shaving the hair, a midline incision of the scalp was made by scissors. The periosteum tissue was removed, the outer skin layers adhered to the skull with tissue adhesive (Vetbond), and the surgical steel head-plate was implanted with dental cement (Prestige Dental Super Bond C+B kit). Mice were then head fixed with the steel head-plate, and areas were marked in the designated stereotactic coordinates for the D1 whisker of the barrel field (3.0 mm lateral from midline and 1.5 mm posterior from bregma). A 3mm diameter craniotomy was performed using a micro drill. The skull was removed gently and intact dura was covered with a drop of cortex buffer. Glass pipettes (tip diameter 10–20 μm connected to a WPI Ultra-microsyringe pump and Micro4 controller (WPI inc. Sarasota USA) were lowered with a micro-positioner (Kopf Instruments) to 200μm DV. The virus solution (200nl) was injected slowly (25nl/min) into the barrel cortex and was composed of virus solution (cre-AAV 1:10000 in equal proportion with GFP-Flex 1:10) mixed with 10% Fast Green for visualisation. Sparse labelling was achieved by using low-titre cre-recombinase and high titre floxed GFP. Rois were chosen at the edge of the virus diffusion radius (usually 150μm radius). The glass pipette was left for a further 2 mins in the brain after injection had finished. In total an injection was completed in 10 mins. A sterile 3mm glass coverslip was placed over the exposed area and sealed with Super Glue and dental cement. Imaging began after a 2- to 3-week recovery period as described previously (Crowe and Ellis-Davies, 2014).

Sensory Manipulation

For sensory deprivation experiments, whiskers of the facial pad contralateral to the cranial window were trimmed by a pair of scissors under a dissection microscope while the mice were under transient isoflurane anaesthesia. Whiskers were subsequently trimmed every other day for the duration of the imaging protocol. Whisker trimming for whole whisker pad deprivation involved trimming all whiskers from the contralateral facial pad (Figure 1A,B), while chessboard pattern deprivation was performed with the D1 whisker always deprived and every other whisker cut with a pair of scissors in a chessboard pattern (Figure 1C,D).

2-photon imaging

For imaging sessions, animals were anesthetized lightly with isoflurane and head fixed via the steel head plate under the objective lens. Two-photon imaging was performed with an Olympus BX68 microscope and PrarieView software. All images were taken with 25x water-immersion objective (Olympus W Plan-APOCHROMAT, 1.05 numerical aperture), 6mm galvo mirrors and a beam expander to ensure maximum illumination of the back-aperture. A mode-locked Ti:sapphire laser (Chameleon Vision S; Coherent) was used to generate two-photon excitation (900nm), with power at the back aperture in the range of 10–50 mW. A pixel dwell time of 8µs with a frame size of 1024 × 1024 pixels was used. Emission wavelengths were band-passed between 525-570nm and the light path included an IR filter. Layer 2/3 neurones were identified by imaging dendrites a minimum of 120 microns from the brain surface, and where possible, tracing basal dendrites back to the cell soma and noting the depth. Dendritic spines on the basal dendrites of layer 2 and layer 3 cells (average depth of soma below dura: 222µm, range: 175-375) were imaged repeatedly every 3 to 4 days over a three-week period before and after deprivation. Dendritic spine images were acquired in 1 µm z-steps. Surface vasculature landmarks in combination with logged coordinates for each region of interest were used for mapping and imaging the same region over the experimental time course. We aimed to image 10 regions of interest from each animal over the period of 3-4 weeks. Two or three baseline images were taken separated by 3 or 4 days (-10, -6, -2 days relative to the day of deprivation at 0). Five post-deprivation time-points were taken at +1,+4, +7, +11 and +14 (Figure 1F).

Photo-lesions

Mice were deeply anaesthetised with isoflurane and head-fixed under the 40x objective lens (Olympus W Plan-APOCHROMAT 0.8 NA water). An optical zoom of x2 was used producing a 50µm x 50µm field of view. The laser was mode locked to a wavelength of 800nM and the Pockels cell adjusted to deliver approximately 50-64 mW power. 2-photon excitation was focused

400 µm below the dura to lesion layer 4. The galvos were centred and the shutter opened for a period of 10-12 mins. Mice were then perfused under terminal anaesthesia and brain sections were stained for cytochrome oxidase to visualise the barrel field and photo-lesions demarcating the imaging field (Figure 1E). Photo-lesions could be seen against the barrel field in horizontal section in layer 4. In more superficial sections the effect was apparent as regions of bleached fluorescence.

Image analysis

ImageJ was used to analyse all images. Raw image stacks were deconvolved using Fiji Deconvolution Lab plugin for Image J from point spread functions taken for the microscope and objective lens used. Images were only analysed where the signal to background intensity was at least 4. For dendritic spine analysis, dendritic spines were classified as a protrusion from the dendritic shaft at least 0.4 µm (Holtmaat et al., 2009). The numbers of spines and dendrites imaged for each genotype and deprivation method can be found detailed in Table 1. Spine formation and elimination rates were calculated by counting the number of gained spines, lost spines, and total spines between each imaging session, per day for each dendrite (Figure 1G,H). Formation rate was calculated by dividing the number of gained spines at each time point by the number of spines present at the first time point. The number formed per day was then calculated based on the interval between observation points. Elimination rate was calculated in an analogous way.

Bifurcating dendrites were chosen randomly in so far as they were not originally sought during image acquisition and were found to be the only ones in our sample that were relatively parallel to the field of view and satisfied our criterion for a bifurcation rather than a smaller offshoot branch. Dendritic width was measured at 3 points way from the bifurcation point and averaged. Where the two branch widths differed by less than 15% we counted them as an even pair of branches.

Spine head size, neck width and neck length were measured for each spine and used to classify spine types. Spine head width was taken as the greatest diameter across the spine head in the image in which it was in focus. Spines were only counted if they protruded at least 0.4µm from the dendrite. Spine head size distributions approximated a log-normal distribution when measured this way (Kolmogorov test) similar to the finding with other methods (Loewenstein et al., 2011). To estimate the error in measuring spine size we took images of dendrites 30 minutes apart and cross-correlated the measures. The method assumes that the spines do not change size greatly over this time period. The average difference in size between observations was less than 0.5% and ranged from 0-11% (mean $\pm$ SD; 0.04% + 0.10%, n=17). The difference in size measured over 30 minutes was therefore approximately 20 times smaller than the average size increase seen with

deprivation. The sum of the residuals for a linear regression fit (y= 1.013x - 0.03) was almost zero (6.2×10^{-3}) suggesting no difference in the population.

We also classified spines according to the major types reported before. Mushroom spines were defined as having a head size >1.15 times the neck width plus a neck length < 0.9 μm. Thin spines were counted as those having a head size >1.15 times the neck width and a neck length >0.9μm. Stubby spines had a neck length < 0.9, and a head size <1.15 times the neck width (in practice very similar neck and head width). We also saw a smaller number of filopodia which were classified as having head size <1.15 times the neck width, but neck length >0.9μm. Filopodia were not included in the spine analysis except where stated in the spine classification sections.

Electrophysiology

Six C57BL/6J mice aged between P87 and P132 (average P104) were deprived of all their whiskers on one side of the snout for 1 day and 4 mice aged between P80 and P152 (average P111) were similarly whisker deprived for 7 days. In addition, 6 mice were deprived in a chessboard pattern for 1 day (P84-97, average P91) and 6 for 7 days (P92-117, average P103). A further 6 undeprived mice were recorded as controls (P75 -P200, average P97). Animals were prepared for spike recording using carbon fibre micro-electrodes under urethane anaesthesia as described before (Armstrong-James and Fox, 1987). Whiskers were acutely trimmed from the spared side of the snout and glued onto the whisker stubs on the deprived side using cyanoacrylate glue. Principal whisker responses were evoked by deflecting the whisker with a fast piezo-electric bimorph stimulator by a standard 1 degree deflection (10ms). Responses were averaged over 50 stimuli and defined as spikes produced during a 3-53ms following stimulation. Details of recording methods can be found elsewhere (Fox, 1992; Fox et al., 2018). Mice were perfused with para-formaldehyde and cryo-protected with sucrose before the brains were flattened for sectioning using a freezing microtome. Sections were reacted for cytochrome oxidase to view the electrolytic lesions made after each recording penetration and thereby establish the principal barrel for each recording penetration and the depth of recording for each cell. Neurones were identified as layer 2/3 or layer 4 and the ratio of the average layer 2/3 to layer 4 response was calculated for each animal. Group averages were calculated for 1 day deprived and 7 day deprived animals and compared with published values for young animals (P28-53) receiving all whisker deprivation for 1 or 7 days.

Experimental Design and Statistical Analysis

The experimental design was longitudinal for spine imaging studies comprising 2 or 3 baseline time points followed by 5 time points over a further two weeks of repeatedly imaging the same locations. This allowed us to apply paired t-tests to compare all possible baseline and post-deprivation time

297 point combinations. Three variants of this statistical approach were planned; one to study another
298 genotype, CaMKII-t286a mice using chessboard deprivation; the other two, to study the effects of
299 whisker deprivation, namely undeprived mice with “chessboard deprived” and “all whisker
300 deprived” mice. Male and female mice were studied for all groups. The ratio of male to female mice
301 was approximately 3:2 respectively in the final sample, due to slightly fewer female mice in the
302 CaMKII-t286a group reaching the weight required for recovery surgery (as stipulated by the animal
303 care legislation under which we operate). We planned to image 10 regions of interest (Roi) for
304 each animal (see Table 1 for summary statistics). However, due to the long period of imaging and
305 the fact that basal dendrites were located deeper than those conventionally studied on apical
306 dendrites, not all Rois remained clear over the full 3 week period. On average, approximately 3
307 Rois remained clear per animal over the full 3 week period (7 or 8 observations for each Roi)
308
309 Spine size changes were analysed using matched pair t-tests as described in the Results section
310 and, where unmatched populations were studied, by ANOVA methods. Spine head sizes were
311 found to be log-normal as described before (Loewenstein et al., 2011), and were therefore log-
312 transformed before using parametric methods. In one case (transient spines in CaMKII-T286A
313 mice), the data was not normally or log-normally distributed and non-parametric tests were used.
314 Spine categorisation analysis and spine lifetime measures were analysed using non-parametric
315 tests (Wilcoxon signed rank and Chi squared methods). Cross-correlations were assessed using
316 linear regression analysis. Data was analysed using JMP software (SAS, Marlow, Bucks UK).
317
318 Precautions were taken against unintended bias: the images were either (a) analysed blind to the
319 hypothesis and/or (b) analysed by more than one person and cross-checked and/or (c) analysed
320 blind to the genotype. In addition, in all cases, a different person to the one collecting and
321 measuring the images performed statistical analysis on the data.
322
323 Electrophysiological data was analysed by averaging neuronal responses to standard whisker
324 deflections for all cells in a given layer for each animal and then averaging values across animals
325 within the treatment/time-point group. Comparisons between groups were then made using
326 ANOVA followed by post-hoc t-tests where appropriate. Population data for formation and
327 elimination rates were also analysed using ANOVA followed by post-hoc t-tests where effects were
328 detected.
329

Results

1. The effect of whisker deprivation pattern on receptive field plasticity

We compared the effects of chessboard pattern deprivation (CWD) and all-whisker deprivation (AWD) on receptive field plasticity in layers 2/3 of the barrel cortex in young adult mice (average age P100).

All whisker deprivation

Depriving all the whiskers uniformly for 1 or 7 days did not cause potentiation of any surround receptive field whisker ($F_{(2,2)}$=1.16, p=0.32), nor indeed change any receptive field component at all (Figure 2A,B). While depriving all the whiskers can cause depression of deprived whisker responses in younger animals (Glazewski et al., 2017), we found it did not produce any change in the receptive fields of the older animals studied here (average age 107 days, range 80-152). The principal whisker response appeared to decrease marginally (to 90% of undeprived values), but was not found to be significantly different from control values ($F_{(1,16)}$=1.44, p=0.25).

Chessboard pattern deprivation

In contrast, chessboard pattern deprivation did cause substantial potentiation of spared whisker responses, both in the barrel-columns where the principal whisker had been deprived ($F_{(2,2)}$=18.66, p<0.001, Figure 2C) and in the spared barrel-columns where the principal whisker had been spared ($F_{(2,2)}$=5.26, p<0.01; Figure 2D). In deprived barrels, the three strongest surround receptive field whisker responses potentiated two to three fold after a single day of deprivation (S1, x2.23; S2, 2.14; S3, 3.03) and increased further by 7 days (S1, x2.75; S2, 3.16; S3, 3.53). In spared barrels, there was a delay to the potentiation, which occurred after 7 days, again for the three strongest surround receptive field whiskers (S1, x2.62; S2, x3.18 S3, x2.91). We also found that principal whisker responses fell to 65% of control values 1-7 days following chessboard pattern deprivation and were significantly different from responses in control undeprived mice ($F_{(1,20)}$ = 6.18, p<0.03).

The difference in effects of CWD and AWD are summarised in Figure 3 (A and D) which show principal whisker responses and the strongest surround whisker responses (S1) for control, 1 day and 7 day deprived mice.

2. The effect of whisker deprivation pattern on spine formation and elimination

To determine whether structural plasticity occurred in layer 2/3 neurones and to see whether it was related to receptive field plasticity observed in layer 2/3 neurones, we repeated the two whisker deprivation patterns in mice prepared with cranial windows for imaging dendritic spines.

All whisker deprivation

We compared the rate of spine formation and elimination in AWD mice with their pre-deprivation baseline rates and found that formation and elimination were unchanged 24 hours after deprivation (baseline versus formation at day 1: $t_{(10)} = 0.45$, $p < .65$; baseline versus elimination at day 1: $t_{(9)} = 0.40$, $p < .69$; paired t-tests) (Figure 3B,C). Similarly, formation and elimination rates were not different from those seen in undeprived animals at any time-point (no effect of deprivation on formation $F_{(1,137)} = 0.068$, p=0.79, or elimination $F_{(1,130)}=0.77$, p=0.38; 2-way ANOVA). This finding is consistent with the lack of functional plasticity found with this deprivation pattern at these ages (Figure 3A) and suggests that spine dynamics are unaffected by a general loss of afferent drive.

Chessboard pattern deprivation

We compared rates of dendritic spine formation and elimination in wild-type mice that had their whiskers deprived in a chessboard pattern with their pre-deprivation baseline rates. We found that formation and elimination increased significantly following 24 hours of deprivation (formation: baseline versus 24h deprivation: $t_{(17)} = 8.75$, $p < .0001$; elimination baseline versus 24h deprivation: $t_{(17)} = 5.10$, $p < 0.0001$; paired t-tests) (Figure 3E). To quantify the effect we compared baseline formation and elimination rates in mice without whisker deprivation over a similar period of time. In undeprived mice at this age (70-125 days), we found that baseline formation and elimination rates were evenly matched, comprising approximately 4% of the original spines per day (Figure 3E). The effect of whisker deprivation was to increase transiently the formation rate to 18% and the elimination rate to 12%. The formation rate then remained elevated above baseline over the succeeding 14 days, though at a far lower rate than that observed on the first day (Figure 3E,F). Repeated measures ANOVA showed a significant two-way interaction between time and deprivation for spine formation in wild-type mice ($F_{(5,163)} = 31.35$, $p < .0001$). When analysed per time-point, the formation rate was significantly elevated on day 1, 4, and 11 ($F_{(1,32)} = 55.93$, $p < .0001$ on day 1, $F_{(1,31)} = 13.15$, $p < .001$ on day 4, $F_{(1,25)} = 13.51$, $p = .005$ at day 11) (Figure 3E).

Elimination rates also remained elevated during CWD, meaning that only a small net gain in spines occurred over the two-week period (Figure 3E). Once again, a repeated measures ANOVA showed a significant two-way interaction between time and deprivation for wild-type mice ($F_{(5,160)}$ = 6.52, p < 0.0001). Analysed per time-point, spine elimination was significantly elevated 1, 4, 7 and 11 days following deprivation, ($F_{(1,32)}$ = 22.91, p < .0001 on day 1, $F_{(1, 31)}$ = 4.77, p < .05 on day 4, $F_{(1,30)}$ = 7.34, p < .05 at day 7, $F_{(1,22)}$ = 9.51, p < .01 at day 11)(Figure 3E). These results show that whisker deprivation patterns that cause functional plasticity (CWD) also cause structural plasticity in layer 2/3 neurones, while whisker deprivation patterns that do not cause functional plasticity (AWD), leave no trace of structural plasticity.

Previous studies have demonstrated that new spines tend to form on a particular subset of dendritic branches that exhibit a naturally high formation rate (Yang et al., 2009). We therefore looked for instances of bifurcating dendrites within our data set. Evenly dividing bifurcations were defined as two daughter branches that differed in width by 15% or less, (average width difference 4%) to distinguish them from minor branches protruding from a main dendrite. We found that both high formation branches (HFB) and low formation branches (LFB) showed significant increases in spine formation 24 hours after chessboard deprivation (HFB $t_{(6)}$=3.33, p<0.02; LFB $t_{(6)}$ = 3.94, p<0.01, paired t-test), although the increase appeared larger for the HFBs (18.7% increase above baseline versus 8.6%), (Figure 4). We compared the behaviour of the HFB and LFB located at bifurcations with individual dendrites that we paired randomly. The HFBs in the random pairs again showed significant increases in spine formation with deprivation (HFB random $t_{(6)}$=4.05, p<0.01 LFB random $t_{(6)}$ = 3.32, p<0.02), paired t-tests), but the difference between HFB and LFB formation rates was smaller than with the natural bifurcating pairs (11.8% increase versus 9.1% increase). Taken across all time-points following deprivation, spine formation was greater in the HFB than the LFB for the bifurcation pairs ($t_{(28)}$ = 3.42, p<0.002, paired t-test), but was not different for the randomly assigned pairs ($t_{(26)}$ =1.3, p=0.2, paired t-test). These findings suggest that while baseline formation rate is predictive of a larger response to deprivation, a particular relationship exists between high and low formation pairs of dendrites at a bifurcation point. In concert with this finding, we found that the absolute rate of spine formation 24 hours after deprivation was moderately well correlated with baseline spine rate for bifurcating pairs of dendrites (r^2=0.45) but not at all for randomly paired dendrites (r^2=0.002) (Figure 4E,F).

Previous studies had not found structural plasticity in layer 2/3 neurones in response to sensory deprivation (Hofer et al., 2009; Ma et al., 2016), but most studies in this area have looked at the apical dendrites rather than the basal dendrites. Apical and basal dendrites receive different afferent input on balance (Petreanu et al., 2009) as shown in Figure 5A. We therefore checked to see whether CWD had similar effects on the apical dendrites compared to the basal dendrites (Figure 5B). We found that 24 hours after deprivation formation and elimination rates were

unaffected by CWD (Figure 5C). Baseline formation rates were similar to that seen on basal dendrites 4.7% (see Table 1) and did not increase significantly following deprivation ($t_{(3)}$ = 0.54, p=0.63, paired t-test). Similarly, elimination rates were similar to those of basal dendrites at 6.1%, and while they appeared slightly higher following deprivation at 8.3%, were not significantly different from baseline measures ($t_{(3)}$ = 1.5, p=0.22, paired t-test). Our results are therefore consistent with previous reports concerning apical dendrites, but additionally show that basal and apical dendrites behave differently under chessboard pattern deprivation.

3. Spine formation and elimination in αCaMKII-T286A mutants

To test whether the increase in spine formation we observe in chessboard deprived wild-type mice is dependent on a cortical LTP-like process, we trimmed whiskers in a chessboard pattern in αCaMKII-T286A point mutants, which have an Alanine substituted at the Threonine 286 location; these animals lack CaMKII auto-phosphorylation (Miller and Kennedy, 1986; Giese et al., 1998) and both cortical LTP in the layer 4 to 2/3 pathway (Hardingham et al., 2003) and cortical experience-dependent potentiation in layer 2/3 (Glazewski et al., 2000). We found that spine formation was unchanged 24 hours following deprivation compared to their baseline pre-deprivation rates (baseline versus formation at day 1: $t_{(11)}$ = 0.177, p < 0.86) (Figure 6). Similarly, there was no difference between formation rates in deprived versus undeprived αCaMKII-T286A mice ($F_{(1,145)}$ = 1.02, p=0.314).

Independent of deprivation, baseline formation and elimination rates were elevated in αCaMKII-T286A mice. Comparison of undeprived animals across all time-points revealed formation rates of 3.8% for wild-types and 4.9% for αCaMKII-T286A mice and these values were significantly different ($t_{(148)}$=12.71, p<0.0005). Similarly, elimination rates were higher in αCaMKII-T286A mice at an average of 4.1% in wild-types versus 4.9% in αCaMKII-T286A mice ($t_{(145)}$=10.87, p<0.002). In these cases, as with others we studied, formation and elimination were closely matched over a timespan of several days, though the equilibrium could be temporarily interrupted by whisker deprivation. However, a striking exception to this rule was found with deprivation of the αCaMKII-T286A mice. Chessboard deprivation increased spine elimination in a similar fashion to that seen in wild-types (compare Figures 3E and Figure 6B, negative values). Spine elimination increased to 15%, 24 hours following deprivation compared to baseline ($t_{(11)}$ = 3.99, p<0.002; paired t-test), though no other time-point was significantly different from undeprived cases. In the absence of spine formation, this transient period of spine elimination produced a net loss of spines that were not replaced over the period of observation.

We also compared formation and elimination rates across wild-type and αCaMKII-T286A mice following chessboard deprivation. We found a significant interaction between time and genotype ($F_{(4,122)}$ = 9.06, p<0.0001) due to a higher formation rate in the wild-types at 1 day and 4 days following deprivation (compare Figures 3E and 6B), ($F_{(1,29)}$ = 26.0, p<0.001 for 1 day and $F_{(1,28)}$ = 6.54, p<0.02 at 4 days). However, ANOVA analysis showed that elimination rates were not different between the two genotypes ($F_{(1,26)}$ = 0.07, p=0.78), even though elimination appeared to last a shorter period after deprivation in αCaMKII-T286A mice. These results show that experience-dependent formation of new spines is dependent on CaMKII auto-phosphorylation, while elimination is not.

4. Spine persistence, spine head size and spine morphology in wild-types

Spine persistence

The new spines that appear on the first day of whisker deprivation in chessboard deprived wild-type mice may either disappear quite quickly or last for some period of time and, in the latter case, they may be capable of forming the substrate for experience-dependent potentiation. To investigate the persistence of new spines, we plotted the rate of spine loss for newly formed spines (i.e. those spines not present in the baseline time period, but which first appeared 24 hours after whisker trimming) (Figure 7A).

Spine lifetimes for new spines were bi-phasically distributed, with transient spines (observed for just a single time-point) and new persistent spines (lasting at least 13 days) dominating the distribution. In undeprived animals, 57% of new spines were transient and just 29% persistent. This pattern was reversed in CWD mice where 29% were transient and 45% persistent. Consequently, the average lifetime of a new spine increased significantly following whisker deprivation ($X^2_{(1)}$=12.7, p<0.0005, n= 188, Wilcoxon test). When coupled with the increased production of spines one day following deprivation, this led to a substantial increase in the proportion of new persistent spines. Over the observation period, approximately 8% of new spines were persistent in chessboard deprived animals compared to less than 1% in undeprived animals (Figure 7A).

Chessboard whisker deprivation creates a mosaic pattern of barrels in the cortex where a barrel that has lost its principal whisker input due to whisker trimming sits next to several barrels with intact principal whisker input (Figure 1D). Electrophysiological measurements of evoked whisker responses showed that potentiation of responses to spared whisker stimulation occurs in deprived barrels and spared barrels (Figure 2C,D). In other words, the spared whisker components of

surround receptive fields are potentiated in general by CWD. In concert with this finding, we observed that the (increased) lifetime of newly formed spines following CWD was identical in the deprived and spared barrels ($X^2_{(1)}$ = 0.74, p=0.38, n=73, Wilcoxon test).

A substantial component of the spines present on the dendrites following deprivation were present in the baseline from the start of observations (Figure 7B). These spines are likely to code for the pre-existing receptive field properties of the neurones, which tend to be dominated by the principal whisker. Given that the principal whisker response decreases following chessboard deprivation, again in deprived and spared barrels (Figure 2) (Wallace and Fox, 1999b), we looked at how spine lifetime was affected by deprivation in this sub-population of spines. We found that whisker deprivation increased the rate of spine loss from the first day of deprivation (Figure 7B). In undeprived animals, the proportion of surviving spines was asymptotic at approximately 65% of the original number after 21 days of observation, suggesting that approximately 65% percent of spines were stable. In chessboard deprived mice, the proportion of surviving spines dropped to 48% over the same observation period, implying an increased loss of at least 17% due to deprivation. Consequently, spine lifetime decreased significantly in chessboard deprived animals for spines already present at the first observation point ($X^2_{(1)}$ = 10.9, p<0.001, n=472, Wilcoxon test) and once again this value was not significantly different between spared and deprived barrels ($X^2_{(1)}$ = 0.24, p=0.62, n=310, Wilcoxon test).

Spine head size for new and eliminated spines

The lifetime of a spine is normally closely related to the size of the spine head, with larger spines exhibiting longer lifetimes than smaller spines (Yasumatsu et al., 2008). We therefore looked at the distribution of spine head sizes of spines newly formed 24 hours after deprivation that persisted for the duration of the CWD period and compared it with the distribution for spines that were present before deprivation and persisted over the whole observation period. We found that the distribution of spine head sizes for new persistent spines (NPS) after 24 hours (Figure 8A) was not significantly different from that for the stable spines that were present throughout the observation period (always present spines, APS; $F_{(1,173)}$=3.13, p=0.07). However, NPS heads were significantly larger than those of transient spines (present for a single time period) ($F_{(1,86)}$=5.76, p<0.02). NPS were also larger than newly formed spines that were subsequently lost over the next 13 days (Figure 8C,D). A two way ANOVA showed an effect of head size on persistence of newly formed spines at 24 hours ($F_{(1, 185)}$ = 3.61, p<0.002), with the difference also apparent at 4, 7 and 11 days following deprivation. These findings suggest that NPS rapidly acquire the same spine head size as the stable population of AP spines after just 24 hours, which prompted us to study spine head size at a briefer 12 hour time-point. We found that spine head sizes for new persistent spines at 12 hours (NPS_{12}) were smaller than those at 24 hours (NPS_{24}) and not different from those of transient spines ($F_{(1,99)}$ =5.05, p<0.01). These results suggest that newly formed spines become established

somewhere between 12 and 24 hours following deprivation (Figure 8C,D).

We also looked at the sizes of spines that become eliminated following whisker deprivation. During the deprivation period, spines that were lost had significantly smaller spine heads than those of the baseline AP population of spines ($F_{(1,296)}$=18.8, p<0.0001) (Figure 8B).

Induced changes in spine head size for stable spines

We were interested to see whether CWD caused a general increase in spine head size, as this might provide a structural substrate for the potentiation of spared whisker responses in addition to the increased numbers of NPSs. When the overall spine population was considered, which included stable and transient populations of spines, we found little overall change in spine size and no statistically significant effects (Figure 9A,C,E). However, spine sizes vary from one time-point to another, due partly to spontaneous spine fluctuations (Yasumatsu et al., 2008) and due partly to the variety of spine lifetimes (and therefore spine sizes) present in any given sample (Figure 8). The AP sub-population of spines, while still showing spontaneous spine fluctuations, were at least free of the variability in spine size due to transient and intermediate spine lifetimes. We therefore tested whether there was an effect of CWD on the AP population of spines. We found that spines in deprived and spared barrels increased in spine head size following deprivation (Figure 9B,D). Within the general population of AP spines, individual spines increased and others decreased in size, but overall the population increased in size (Figure 9D).

There was a clear relationship between the size of the spines at baseline at its direction of size change following deprivation (Figure 9F). The small spines tended to show increased head sizes while the larger spines showed decreased head sizes. This effectively provided an apparent homeostatic reaction to the CWD induced enlargement seen in the stable spine population. The increase in the population spine head size was therefore due to many small spines increasing and only being partly compensated by fewer large spines decreasing in head-size.

The change in spine size was relatively small (on average 10%). Nevertheless, the AP spines represent some 65% of the total spine population at any one time (dependent on age) and the general effect may therefore be physiologically significant. We found no difference in spine size between the control period baseline time-points ($t_{(147)}$=1.13, p=0.26), but all the baseline time-points differed from all the post-deprivation time-points (for example at 1 day post-deprivation, $t_{(147)}$=4.05, p<0.0001, matched pair t-test; see Figure 9 legend for full statistics).

We also looked to see if apical dendrites also showed increases in the size of the stable spine population following CWD. We found that unlike basal dendrites, the stable spine population on the

apical dendrites showed no change in population spine size 24 hours following deprivation ($t_{(97)}$ =0.76, p=0.44, matched pair t-test) (Figure 5D). It was also apparent that the average size of the apical dendrite spine heads was in general smaller those of basal dendrites when comparing baseline measures with undeprived controls over a similar period of time ($F_{(1, 589)}$=11.8, p<0.001).

We also tested to see whether the AP population of spines changed size in the AWD mice. In contrast to the effect of CWD, we found that AWD produced a small decrease in average spine size (Figure 9B). Overall, AWD reduced AP spine head size to 94% of control values over the deprivation period and this was a significant effect ($F_{(1,1285)}$ = 4.03, p<0.0002). The effect was clearer from 7 days onward and AP spine head sizes averaged 90% of control values after 14 days of AWD ($t_{(137)}$=3.43, p<0.0005, matched pair t-test).

Spine Morphology

We classified spines into one of four types, mushroom spines, thin spines, stubby spines and filopodia (see Methods) using previously published criteria (Grutzendler et al., 2002; Oray et al., 2006; Rodriguez et al., 2008). In the general population of all spines, we found that most spines were thin (61%), many were mushroom (16%) and a few were filopodia (9%) (see Table 2). The rest were classified as apparently stubby spines, where the neck was short and appeared to be of similar size to the head (14%).

We found that the NPS population differed in morphology from the general population, even after 14 days of CWD, comprising fewer mushroom spines (5% versus 16%) and more stubby spines and filopodia ($X^2_{(9)}$ = 63, p<0.001; see Table 2). This suggests that it takes longer than 14 day for most of the very largest spine types to become established from genesis. We also looked at the stable population of AP spines and found that they progressively lost mushroom spines over the 14 day post-deprivation period from 16% to 2% by day14 ($X^2_{(9)}$ = 40, p<0.001; see Table 2), being replaced mostly with thin and stubby spine types. If one assumes that the principal whisker probably transmits via mushroom spines in its principal barrel, this finding is in keeping with the physiological data showing that principal whisker responses decrease with chessboard deprivation. It is also in keeping with the general finding that larger spines tend to decrease and smaller spines increase in size with deprivation (Figure 9F). On average, a small increase in spine head size in the AP population occurs with CWD (Figure 9B,D) accompanied by a reduced number of mushroom spines.

5. Spine persistence, spine head size and spine morphology in αCaMKII-T286A mutants

Spine persistence

Given the relationship between spine lifetime and spine size, we tested whether the higher baseline formation and elimination rates present in αCaMKII-T286A mice resulted in shorter spine lifetimes in general and whether the size of the spines was subsequently different. Indeed, spine lifetimes were found to be briefer in αCaMKII-T286A mutants compared to wild-types (Figure 10A). A two way ANOVA showed an effect of deprivation and genotype on spine lifetime but no interaction between the two ($F_{(3,1059)}$ = 7.65, p<0.0001). In undeprived αCaMKII-T286A mutants, spines that were already present from the first observation point were eliminated at a faster rate than in wild-types (Figure 10A; $X^2_{(1)}$ = 7.0, p<0.01, n = 511, Wilcoxon test) falling to 50% of the original number over 20 days. This is consistent with the observation that baseline spine formation and elimination is higher in αCaMKII-T286A animals than in wild-types. The rate of spine loss was increased further by deprivation (Figure 10A; $X^2_{(1)}$= 8.8, p<0.003, n = 588, Wilcoxon test) and resulted in just 38% of spines persisting for 20 days. Neither decay curves for surviving spines in deprived nor undeprived animals reached an asymptote over the period of observation (Figure 10A). Spine loss was approximately 12% greater in deprived αCaMKII-T286A mice than in undeprived control cases after 14 days of CWD. These observations are consistent with the electrophysiological evidence, which shows that CWD causes depression of deprived whisker responses in αCaMKII-T286A mice but no potentiation of spared whisker responses (Hardingham et al., 2003).

Spine lifetime for new spines produced 24 hours following deprivation were similar to those of wild-types. However, the number of new spines formed after deprivation were no greater than at any other time-point (Figure 10B), which meant that after 14 days of deprivation, the number of spines formed 24hours after deprivation was 1.3% of the total and not significantly different from the number expected in undeprived αCaMKII-T286A mutants of 0.8% (Figure 10B).

Spine head size for new and eliminated spines

We compared new persistent spines (NPS) formed on the first day following deprivation with spines that were stable and always present (AP) throughout the entire observation period in undeprived animals. We found that just as with wild-types, NPSs had the same size spines heads as the AP population in αCaMKII-T286A mice (Figure 10D). However, spine heads of all types were generally smaller than in wild-types. A two way ANOVA showed an effect of genotype but not

of spine type (AP versus NP) across wild-types and αCaMKII-T286A mutants ($F_{(3,394)}$=4.88, p<0.003). Post hoc test showed that this was because persistent spine heads were significantly smaller in αCaMKII-T286A mutants than in wild-types $t_{(393)}$= 3.29, p<0.002. This conclusion was strengthened when we further tested whether spine head sizes were different in undeprived wild-types and αCaMKII-T286A mutants (Figure 10 E,F) and found they were ($t_{(1281)}$= 6.89, p<0.0001).

We also compared the size of transient spines with the persistent spine population and found once again that, as with wild-types, transient spines were significantly smaller than persistent spines (χ^2 = 68.75, p<0.0001). These findings suggest that spine head size is an important determinant of spine stability in αCaMKII-T286A mutants just as in wild-types, but that the critical size for stability is smaller in αCaMKII-T286A mutants.

Changes in spine head size for initially present spines

As described above, we found that in wild-types, the AP population of spines showed a small but significant increase in spine head size following deprivation. We found no comparable change in αCaMKII-T286A mice however (Figure 11A,B) and the average spine sizes for the population of AP spines were not different from any pair of baseline to post-deprivation comparisons (for example baseline to day 1 $t_{(86)}$=1.04, p=0.299; Figure 11). However, just as with the wild-type cases, individual spines in the αCaMKII-T286A mice showed increases and decreases in spine size from one time-point to another (Figure 11C). Consistent with spine fluctuation analysis, the smaller spines tended to increase in size and the larger spines decrease in size (Figure 11D), but overall the spine head size distribution remained unchanged by deprivation. The effect of fluctuations are therefore not dependent on CaMKII auto-phosphorylation. However, because the spontaneous increases in spine size within the population are small compared with those in wild-types (due to a lack of potentiation in these animals), the fluctuation range is also smaller and the spine population settles to a smaller average spine head size (Figure 11A,C,D).

Spine Morphology

The distribution of spine types found in undeprived αCaMKII-T286A mice was different from that seen in wild-types, with fewer mushroom spines (6.5%), and more thin spines (87%) (see Table 2; $X^2_{(3)}$=64.5, p<0.0001). This result is in keeping with the general finding that spine head sizes were smaller in αCaMKII-T286A mice than in wild-types, which may be related to their lack of LTP and may thereby give rise to their higher basal levels of spine elimination.

Discussion

This study shows that layer 2/3 neurones do undergo structural plasticity in the barrel cortex, but (a) only under conditions that produce functional plasticity of receptive field structure (CWD not AWD) and (b) only on the basal and not the apical dendrites. Why does CWD cause functional and structural plasticity while AWD does not? CWD alters the natural timing of activity in columnar and trans-columnar circuits driven by spared and deprived whiskers and therefore creates the conditions for spike-timing dependent potentiation and depression (Wallace and Fox, 1999a; Celikel et al., 2004). The spared whiskers can also provide activity for non spike-timing forms of LTP in barrel cortex (Gambino and Holtmaat, 2012). Neither of these contingencies are created by AWD, which leads to a uniform decrease in activity levels and consequently little opportunity for Hebbian forms of plasticity. At the ages studied here, neither does AWD cause homeostatic plasticity (compare Figure 2B with (Glazewski et al., 2017)). In common with the visual cortex (Ranson et al., 2012), barrel cortex appears to exhibit homeostatic plasticity in young rather than adult animals.

Our findings may help to explain earlier studies that did not observe structural plasticity in layer 2/3 cortical neurones. Studies in barrel cortex where all the whiskers were deprived uniformly also reported a lack of rapid structural plasticity in layer 2/3 neurones (Zuo et al., 2005; Ma et al., 2016). Studies in visual cortex, where activity was uniformly decreased in the monocular zone by contralateral eye-enucleation, also found a lack of structural plasticity in layer 2/3 (Barnes et al., 2015). One study in binocular visual cortex did use monocular deprivation however, which would be expected to create activity contrasts between ipsi- and contra-lateral eye inputs. In this case, no structural plasticity was found on the layer 2/3 neurones (Hofer et al., 2009), possibly because the apical dendrites were studied rather than the basal dendrites.

Why do the basal dendrites exhibit plasticity while the apical dendrites do not? A possible explanation may lie in their different inputs. Basal dendrites tend to receive feedforward sensory input from layer 4 and to some extent directly from the thalamus (White, 1978; Petreanu et al., 2009; Hooks et al., 2011; Mao et al., 2011). Apical dendrites tend to receive feedback connections from other cortical areas including motor cortex (Petreanu et al., 2009). Therefore, sensory deprivation is more likely to affect feedforward connections onto basal dendrites while motor tasks are more likely to affect feedback connections onto apical dendrites. In favour of this theory, apical dendritic plasticity does occur in motor tasks requiring mice to move their whiskers accurately to receive a reward (Kuhlman et al., 2014).

One further level of dendritic specialisation was observed in this study. We found that new spine formation tended to be greater following whisker deprivation at dendritic branches with a naturally higher basal turnover rate, confirming findings of (Yang et al., 2014) and colleagues. This suggests that even among basal dendrites, some are primed to undergo plasticity and some are not.

Dual-component structural plasticity

Chessboard pattern deprivation causes potentiation of spared whisker responses and depression of deprived whisker responses (Wallace and Fox, 1999b). Spared whisker potentiation correlates with an increase in new persistent spines, but also a small but significant increase in spine head size of the stable (AP) spine population. Most layer 2/3 neurones in the barrel cortex receive multi-whisker input (Armstrong-James and Fox, 1987) and therefore, theoretically, only need to strengthen pre-existing synapses rather than to create new ones. Nevertheless, new spines *are* produced and since they stabilise over a period of two weeks, are thought to make functional synapses (Knott et al., 2006). It is therefore likely that new persistent spines represent the second component of the dual-component structural plasticity mechanism. Neither, AP enlargement nor NPS formation are present in the CaMKII-T286A mutants, which also lack experience-dependent potentiation (Glazewski et al., 2000) and cortical LTP (Hardingham et al., 2003), providing further evidence that functional plasticity depends on the observed structural plasticity. A similar conclusion on NPS formation has been reached before for CWD induced potentiation of spared whisker responses and layer 5IB apical dendrites in barrel cortex (Wilbrecht et al., 2010), however, we believe the CaMKII auto-phosphorylation dependent AP spine enlargement is an entirely new observation.

The Effect of Intrinsic Spine Fluctuations

Within the stable spine population, we found that smaller spines increased and the larger spines tended to decrease in size between time-points. This provides a self-regulatory homeostatic response to potentiation. Spine fluctuation analysis shows that spine sizes tend to spontaneously change this way in the absence of overt Hebbian processes to direct changes in spine size (Yasumatsu et al., 2008) and indeed lead to the log-normal spine head size distribution observed here and in other studies (Loewenstein et al., 2011). Theoretical studies have shown that Hebbian processes combined with random spine fluctuations creates an intrinsically homeostatic system (Matsubara and Uehara, 2016).

The increase in size of the stable spine population following CWD is reminiscent of a TNF-alpha dependent homeostatic increase in spine size seen in dendrites that show elevated spine elimination (Barnes et al., 2017). However, two arguments suggest that the size increase we saw

is not homeostatic; first, because the AP spine enlargement occurs against a background of increased spine formation rather than a loss of spines, which suggests that there is no loss for the homeostatic mechanism to compensate. Second, the AP spine enlargement was absent in the αCaMKII-T286A point mutants, which lack LTP but not TNF-alpha dependent homeostatic plasticity (Greenhill et al., 2015). This suggests that AP spine enlargement is related to Hebbian addition and input specific potentiation rather than a homeostatic mechanism. This fits with the neurophysiological effect of chessboard deprivation, which is to increase selectively the spared whisker responses rather than homeostatically increase whisker responses in general (Wallace and Fox, 1999b; Hardingham et al., 2008).

The role of CaMKII in structural plasticity

Spine heads fluctuate in size independent of activity driven increases and decreases in spine size (Yasumatsu et al., 2008). Consequently, spines with small heads are vulnerable to elimination from spontaneous decreases in spine size. New spines are vulnerable to elimination for this reason and we found that they only persist if their heads grow rapidly to the population average size. Spine head size for new persistent spines is indistinguishable from the main population of stable spines after 24 hours in wild-type mice, while new spines that are eliminated are smaller, like transient spines in general. Activity-dependent spine enlargement requires CaMKII (Bosch et al., 2014; Hedrick et al., 2016; Fu and Ip, 2017). The lack of CaMKII auto-phosphorylation in the αCaMKII-T286A mice, presumably prevents sensory directed spine enlargement and stabilisation, therefore new spines tend to be eliminated more frequently in αCaMKII-T286A mice leading to their baseline turnover rate being about 24% higher than in wild-types.

In addition to the decreased persistence of new spines, we also found that new spines do not form at an elevated rate following CWD in αCaMKII-T286A mice. This suggests that αCaMKII-autophosphorylation is required for the substantial increase in new spine formation itself. In favour of this theory, it has been shown that CaMKII lies at the centre of several signalling pathways in the spine head, one of which leads to production of RhoA, which can diffuse to neighbouring spines and thereby affect the cytoskeleton of new and emerging spines and another that generates local BDNF synthesis, trkB signalling and diffusion of newly activated Rac1 to neighbouring spines with a similar effect (Hedrick et al., 2016). Both Rac1 and RhoA are part of the system that leads to spine enlargement via LIMk translocation to and binding of cofilin to the spine head (Bosch et al., 2014). However, it is not clear at this stage whether this system alters the dendritic cytoskeleton in such a way as to initiate new spine production, rather than increasing the probability of spontaneously occurring new spines becoming stabilised by spine head enlargement.

Conclusions

We draw a number of conclusions from the present findings; first, that Layer 2/3 neurones do show robust structural plasticity in response to whisker deprivation and therefore the functional plasticity we see in this layer is likely to depend on underpinning structural plasticity. Previous studies may have missed this by looking at other dendritic locations or by using an ineffective whisker deprivation method. Second, that potentiation occurs due to a dual-component enlargement of stable spines plus addition of new spines and CaMKII is central to both. While the role of CaMKII in LTP and spine enlargement is reasonably well understood, the mechanism by which it is involved in spine production is not established at present.

Figure Legends

Figure 1. Whisker deprivation patterns and spine tracking.
A: Unilateral all whisker deprivation (AWD), which produces **B**: uniform deprivation of all barrels in the cortex. **C**: Unilateral Chessboard pattern whisker deprivation (CWD) produces **D**: a chessboard pattern of active and deprived barrels whereby every barrel deprived of its principal whisker (light grey) is surrounded by four barrels that have their principal whisker intact (dark grey) and vice versa. **E**: Photo-lesion are made in layer 4 of the barrel cortex on the last day of imaging (black arrows), to co-register the regions of interest within which spines are imaged with their corresponding home barrels. **F:** Imaging time points relative to deprivation on time-point zero were -10, -6, -2, +1, +4, +7, +11 and +14 days. In some cases 12 and 24 hour time points were taken. **G**: Spines are tracked over a period of days, shown here for 6 days before deprivation (-6), two days before (-2) and 4 days after deprivation (+4). Note that spine number 17 is branched: such cases were counted as one spine. Some spines are eliminated from one time point to the next (red numbering), others are formed anew (green numbering). **H**: Examples of eliminated (red arrows) and newly formed or enlarged spines (green arrows) shown for a dendrite imaged at 2 days before and 7 days after deprivation. Yellow arrow indicates a spine where the spine head shrinks over this period. Calibration bars are 150 μm (E), and 5 μm (G and H).

Figure 2. Effect of deprivation pattern on receptive field properties.
A: Principal whisker and surround receptive field (SRF) whiskers are plotted against the response evoked in layer 2/3 averaged across animals. SRF responses are ranked for each cell (S1, S2 …S6) before averaging across cells for each animal. Inset: diagram of barrel field indicates all barrels receive principal whisker input (dark grey). **B**: Receptive field properties are unchanged in animals unilaterally deprived of all their whiskers at 1 day (grey) and 7 days (black) post-deprivation. Inset: diagram of barrel field shows all barrels are deprived of principal whisker input (light grey). **C**: Receptive fields in barrels deprived of principal whisker input are altered by chessboard pattern deprivation (CWD). In deprived barrels, spared surround whisker responses (S1-6) increase while principal whisker (PW) responses decrease. Inset: diagram of barrel field shows that barrels deprived of their principal whisker (orange) alternate with barrels with their spared whisker intact (dark grey). **D**: Receptive fields in barrels with spared principal whiskers also show an increase in surround whisker responses at 7 days but not 1 day. Inset: green represents spared barrels and light grey deprived barrels.

Figure 3. Effect of deprivation pattern on spine formation and elimination.
A: All whisker deprivation (AWD) evenly deprives the barrel field of its principal whisker input and does not significantly alter principal whisker responses (white bars), nor the strongest (S1) spared

surround whisker responses (black bars) after 1 or 7 days of deprivation. **B**: Similarly, AWD does not affect spine formation (black bars) or elimination (black bars, plotted as negative values for clarity), which remain constant following deprivation compared with formation and elimination in undeprived animals (white bars). **C**: Therefore, AWD cumulative formation (blue line) and elimination curves (red line) entirely overlap with those for undeprived cases (see key). **D**: Chessboard pattern deprivation (CWD) results in alternate deprived and spared barrels in the cortex (diagram; spared barrels dark grey) and causes potentiation of spared whisker responses in deprived barrels (black bars) and principal whisker responses to depressed (white bars). **E**: Similarly, CWD causes spine formation and elimination to increase significantly 1 day following deprivation and remain elevated for at least 11 days following deprivation compared to undeprived values (*** $p<0.001$, ** $p<0.01$, * $p<0.05$). **F:** Consequently, cumulative spine formation is increased over 14 days to approximately 90% of the originally present spines (blue line) compared to approximately 40% in undeprived animals (green line). Cumulative spine elimination in CWD (red line) is similar to formation over 14 days and significantly higher than in undeprived animals (purple line).

Figure 4. Effect of basal formation rate on chessboard pattern whisker deprivation induced formation rate in bifurcating dendrites and randomly paired singly assayed dendrites. **A:** Bifurcating dendrites: the high formation branches (HFB, solid lines, black diamonds) from the bifurcation pair are defined from their baseline formation rate and show a greater reaction to deprivation than low formation branches (LFB, dashed lines, open squares). The plot shows the cumulative spine formation with time. **B:** Random pairs: HFBs from randomly paired branches appear to show a greater reaction to deprivation but this is not significantly different from the LFB random pair. **C:** Bifurcating pairs: formation rate plotted in histogram format showing rates assayed per time point for HFBs (black bars) and LFBs (white bars). **D:** Random pairs: formation rates for randomly paired dendrites. **E:** Cross-correlation between basal formation and deprivation induced formation rates in bifurcation dendrite pairs. Basal formation is broadly predictive of deprivation induced formation ($r^2=0.45$) and is highly significant (see Results section). **F:** Basal formation rate is not predictive of deprivation induced formation rate for randomly assigned pairs of dendrites ($r^2=0.00195$).

Figure 5. Lack of effect of chessboard pattern deprivation on measures of synaptic plasticity on apical dendrites in barrel cortex.

A: Diagram of barrel cortex showing the inputs to apical dendrites in layer I (LI) and the different inputs to basal dendrites in layers 2 (L2) and layer 3 (L3). Inputs to apical dendrites arise from other cortical areas such as secondary somatosensory cortex (S2) and primary motor cortex (M1) as well as the medial part of the posterior thalamic nucleus (POm). Basal input arise from layer 4 cells and other layer 2/3 cells as well as some direct VPm input onto layer 3 cells. **B:** (i) Low power image of apical dendrites in L1 (scale bar =) (ii- iv) descending sequence of images from 30-180

microns below the dura (scale bar in iv is 30μm). **C:** The cumulative spine formation rate is shown for baseline time-points and for 1 day (24 hours) after chessboard whisker deprivation. The plot does not show an increase in slope 1 day after deprivation that would be characteristic of increased spine formation and is seen with CWD for basal dendrites (compare with 3F and 4A,B). **D:** The spine sizes of the stable (AP) population of spines were calculated for each time-point and show no change post-deprivation (compare with Figure 9B for basal dendrites).

Figure 6. Lack of effect of chessboard pattern deprivation on spine formation in αCaMKII-T286A homozygous mice.

A: Diagrammatic representation of the chessboard deprived pattern. **B:** Chessboard pattern deprivation (black bars) does not cause an increase in spine formation (positive values) above baseline (white bars) following deprivation. However, spine elimination (plotted as negative values for clarity) is increased on the first day following whisker deprivation (black bars) relative to undeprived CaMKII-T2286A (white bars) (* $p<0.05$). **C:** Cumulative formation curves overlap for deprived (blue line) and undeprived (green line) αCaMKII-T286A mice and are not different, while cumulative spine elimination (red line) increases one day after deprivation but returns to basal rates thereafter.

Figure 7. Effect of chessboard whisker deprivation on lifetime of newly formed and already present spines.

A: Newly formed spines in CWD wild-type mice (blue line) comprise 18% of initially present spines one day following deprivation. The new spine count decays with time to asymptote at approximately 8% by 14 days of deprivation. New spines in undeprived wild-types only comprise 4% of the total on any given day and decay to approximately 1% over the same time period (black line). **B:** Spines already present at the first observation time-point naturally decay over time in undeprived animals (black line) to asymptote at approximately 65% of the population after 20 days. Chessboard pattern deprivation (onset shown by arrow) increases the rate of decay (green line) by approximately 18% over the same period. NB: spines summed across all cases in each group.

Figure 8. Relationship between spine size and lifetime for eliminated, transient and new persistent spines in wild-types.

A: New spines formed after chessboard deprivation that persist (blue line) have the same spine head size distribution 24 hours after deprivation as the stable spine population (black line). **B:** Spines that are eliminated one time-point following observation of their presence (green line) are smaller than the stable spine population (black line). **C:** The average spine head size of the stable spine population for undeprived wild-types is plotted over a three week period (grey line, mean and sem). Transient spines (present for a single time point) have smaller average spine head sizes (red triangles). Average head size of new persistent spines (blue line) increase rapidly between 12 and

24 hours of chessboard whisker deprivation to exceed transient spine head sizes at 24 hours and are indistinguishable from the stable spine sizes after 4 days. **D:** Cumulative distribution functions for the spine head sizes of transient (red), new persistent at 12 hours (light blue), new persistent at 24 hours (dark blue) and stable spines (black) shown in **C**.

Figure 9. The effect of deprivation pattern on spine size of the stable spine population in wild-types.

A: The overall spine head size in the general population of all spines does not change with CWD. However, **B:** the average spine head size does increase in the population of always present spines with CWD (blue line), though not AWD (grey line). **C:** Cumulative distribution functions for the general population of all spines before (red) and after deprivation (green) are similar (note that red and green lines correspond to red and green time-points in **A**). **D:** However, the cumulative distribution function for the stable spine population shifts right (larger values) from baseline (red) after chessboard pattern deprivation (green). Log transformed spine size distributions for each time point were compared using matched pair-t-tests. Baseline time-points were not different ($t_{(147)}$=1.13, p=0.26), while baseline and day 1, 4, 7, 11 and 14 were different ($t_{(147)}$=4.0,p<0.0001; $t_{(147)}$=4.44, p<0.0001; $t_{(147)}$=3.63, p<0.0004; $t_{(147)}$=2.50, p<0.013; $t_{(147)}$=2.3, p<0.022) respectively. **E**: The change in spine head size is related to the original size of the spines and is shown for the general population of spines in **E** and for the stable spines only in **F**. Note that newly formed spines appear on the y-axis and eliminated spines appear along x = -y. **F:** Spine larger than about 1 μm tend to decrease in size while those smaller than 1 μm increase in size.

Figure 10. Effect of chessboard whisker deprivation and the αCaMKII-T286A genotype on lifetime of newly formed and already present spines.

A: The survival fraction plot shows that spine lifetimes are briefer in αCaMKII-T286A mice (black line) compared to wild-types (grey line). Chessboard pattern deprivation decreases spine survival further in αCaMKII-T286A mice (green line). **B:** Newly formed spines show similar persistence in chessboard deprived and undeprived αCaMKII-T286A mice. **C:** The distribution of spine head sizes is smaller for spines eliminated at the next time point (green line) compared to stable spines (black line). **D**: Newly formed spines that persist (blue line) have a similar spine size distribution to that of stable spines (black line) in αCaMKII-T286A mice. **E**: Spine head sizes are smaller in αCaMKII-T286A mice (red) compared to wild-types (black); data for undeprived animals. **F**: Cumulative distribution function for data shown in **E**. NB: Spines are summed for all cases within each group to form the decay curves.

Figure 11. The effect of deprivation pattern on spine size of the stable spine population in αCaMKII-T286A mice.

A: Chessboard pattern deprivation leads to an increase in the average spine head size in the stable spine population in wild-types (blue line) but not in the αCaMKII-T286A mutants (green line). **B:** In αCaMKII-T286A mutants, the cumulative distribution functions of spine head size overlap for the stable spine population before (red line) and after chessboard pattern deprivation (blue). **C:** Trajectories of individual spine size changes between baseline and 1 day post chessboard-deprivation. **D:** For the stable population, small spine heads tend to increase in size and large spine heads decrease in αCaMKII-T286A mice, but the overlap in sizes increasing and decreasing is greater in αCaMKII-T286A mice than with wild-types (compare with Figure 9F). Data in **D** is for the same population shown in **C** and **B**.

References

Armstrong-James M, Fox K (1987) Spatiotemporal convergence and divergence in the rat S1 "barrel" cortex. J Comp Neurol 263:265-281.

Barnes SJ, Sammons RP, Jacobsen RI, Mackie J, Keller GB, Keck T (2015) Subnetwork-Specific Homeostatic Plasticity in Mouse Visual Cortex In Vivo. Neuron 86:1290-1303.

Barnes SJ, Franzoni E, Jacobsen RI, Erdelyi F, Szabo G, Clopath C, Keller GB, Keck T (2017) Deprivation-Induced Homeostatic Spine Scaling In Vivo Is Localized to Dendritic Branches that Have Undergone Recent Spine Loss. Neuron 96:871-882 e875.

Bosch M, Castro J, Saneyoshi T, Matsuno H, Sur M, Hayashi Y (2014) Structural and molecular remodeling of dendritic spine substructures during long-term potentiation. Neuron 82:444-459.

Celikel T, Szostak VA, Feldman DE (2004) Modulation of spike timing by sensory deprivation during induction of cortical map plasticity. Nat Neurosci 7:534-541.

Chang JY, Parra-Bueno P, Laviv T, Szatmari EM, Lee SR, Yasuda R (2017) CaMKII Autophosphorylation Is Necessary for Optimal Integration of Ca(2+) Signals during LTP Induction, but Not Maintenance. Neuron 94:800-808 e804.

Chen BE, Lendvai B, Nimchinsky EA, Burbach B, Fox K, Svoboda K (2000) Imaging high-resolution structure of GFP-expressing neurons in neocortex in vivo. Learn Mem 7:433-441.

Crowe SE, Ellis-Davies GC (2014) Longitudinal in vivo two-photon fluorescence imaging. J Comp Neurol 522:1708-1727.

Dachtler J, Hardingham NR, Glazewski S, Wright NF, Blain EJ, Fox K (2011) Experience-dependent plasticity acts via GluR1 and a novel neuronal nitric oxide synthase-dependent synaptic mechanism in adult cortex. J Neurosci 31:11220-11230.

Fox K (1992) A critical period for experience-dependent synaptic plasticity in rat barrel cortex. J Neurosci 12:1826-1838.

Fox K (1994) The cortical component of experience-dependent synaptic plasticity in the rat barrel cortex. J Neurosci 14:7665-7679.

Fox K, Wong RO (2005) A comparison of experience-dependent plasticity in the visual and somatosensory systems. Neuron 48:465-477.

Fox K, Greenhill S, Haan Ad (2018) Chapter 10 - Barrel Cortex as a Model System for Understanding the Molecular, Structural, and Functional Basis of Cortical Plasticity: Elsevier.

Fu AK, Ip NY (2017) Regulation of postsynaptic signaling in structural synaptic plasticity. Curr Opin Neurobiol 45:148-155.

Gambino F, Holtmaat A (2012) Spike-timing-dependent potentiation of sensory surround in the somatosensory cortex is facilitated by deprivation-mediated disinhibition. Neuron 75:490-502.

Giese KP, Fedorov NB, Filipkowski RK, Silva AJ (1998) Autophosphorylation at Thr286 of the alpha calcium-calmodulin kinase II in LTP and learning. Science 279:870-873.

Glazewski S, Fox K (1996) Time course of experience-dependent synaptic potentiation and depression in barrel cortex of adolescent rats. J Neurophysiol 75:1714-1729.

Glazewski S, Greenhill S, Fox K (2017) Time-course and mechanisms of homeostatic plasticity in layers 2/3 and 5 of the barrel cortex. Philos Trans R Soc Lond B Biol Sci 372.

Glazewski S, Giese KP, Silva A, Fox K (2000) The role of alpha-CaMKII autophosphorylation in neocortical experience-dependent plasticity. Nat Neurosci 3:911-918.

Greenhill SD, Ranson A, Fox K (2015) Hebbian and Homeostatic Plasticity Mechanisms in Regular Spiking and Intrinsic Bursting Cells of Cortical Layer 5. Neuron 88:539-552.

Grutzendler J, Kasthuri N, Gan WB (2002) Long-term dendritic spine stability in the adult cortex. Nature 420:812-816.

Hardingham N, Wright N, Dachtler J, Fox K (2008) Sensory deprivation unmasks a PKA-dependent synaptic plasticity mechanism that operates in parallel with CaMKII. Neuron 60:861-874.

Hardingham N, Glazewski S, Pakhotin P, Mizuno K, Chapman PF, Giese KP, Fox K (2003) Neocortical long-term potentiation and experience-dependent synaptic plasticity require alpha-calcium/calmodulin-dependent protein kinase II autophosphorylation. J Neurosci 23:4428-4436.

Hedrick NG, Harward SC, Hall CE, Murakoshi H, McNamara JO, Yasuda R (2016) Rho GTPase complementation underlies BDNF-dependent homo- and heterosynaptic plasticity. Nature 538:104-108.
Hofer SB, Mrsic-Flogel TD, Bonhoeffer T, Hubener M (2009) Experience leaves a lasting structural trace in cortical circuits. Nature 457:313-317.
Hoffman KL, McNaughton BL (2002) Coordinated reactivation of distributed memory traces in primate neocortex. Science 297:2070-2073.
Holtmaat A, Wilbrecht L, Knott GW, Welker E, Svoboda K (2006) Experience-dependent and cell-type-specific spine growth in the neocortex. Nature 441:979-983.
Holtmaat A, Bonhoeffer T, Chow DK, Chuckowree J, De Paola V, Hofer SB, Hubener M, Keck T, Knott G, Lee WC, Mostany R, Mrsic-Flogel TD, Nedivi E, Portera-Cailliau C, Svoboda K, Trachtenberg JT, Wilbrecht L (2009) Long-term, high-resolution imaging in the mouse neocortex through a chronic cranial window. Nature protocols 4:1128-1144.
Hooks BM, Hires SA, Zhang YX, Huber D, Petreanu L, Svoboda K, Shepherd GM (2011) Laminar analysis of excitatory local circuits in vibrissal motor and sensory cortical areas. PLoS biology 9:e1000572.
Jacob V, Petreanu L, Wright N, Svoboda K, Fox K (2012) Regular spiking and intrinsic bursting pyramidal cells show orthogonal forms of experience-dependent plasticity in layer V of barrel cortex. Neuron 73:391-404.
Josselyn SA, Frankland PW (2018) Memory Allocation: Mechanisms and Function. Annu Rev Neurosci 41:389-413.
Keck T, Keller GB, Jacobsen RI, Eysel UT, Bonhoeffer T, Hubener M (2013) Synaptic scaling and homeostatic plasticity in the mouse visual cortex in vivo. Neuron 80:327-334.
Knott GW, Holtmaat A, Wilbrecht L, Welker E, Svoboda K (2006) Spine growth precedes synapse formation in the adult neocortex in vivo. Nature neuroscience 9:1117-1124.
Kuhlman SJ, O'Connor DH, Fox K, Svoboda K (2014) Structural plasticity within the barrel cortex during initial phases of whisker-dependent learning. J Neurosci 34:6078-6083.
Lendvai B, Stern EA, Chen B, Svoboda K (2000) Experience-dependent plasticity of dendritic spines in the developing rat barrel cortex in vivo. Nature 404:876-881.
Loewenstein Y, Kuras A, Rumpel S (2011) Multiplicative dynamics underlie the emergence of the log-normal distribution of spine sizes in the neocortex in vivo. J Neurosci 31:9481-9488.
Ma L, Qiao Q, Tsai JW, Yang G, Li W, Gan WB (2016) Experience-dependent plasticity of dendritic spines of layer 2/3 pyramidal neurons in the mouse cortex. Developmental neurobiology 76:277-286.
Mao T, Kusefoglu D, Hooks BM, Huber D, Petreanu L, Svoboda K (2011) Long-range neuronal circuits underlying the interaction between sensory and motor cortex. Neuron 72:111-123.
Matsubara T, Uehara K (2016) Homeostatic Plasticity Achieved by Incorporation of Random Fluctuations and Soft-Bounded Hebbian Plasticity in Excitatory Synapses. Frontiers in neural circuits 10:42.
Miller SG, Kennedy MB (1986) Regulation of brain type II Ca2+/calmodulin-dependent protein kinase by autophosphorylation: a Ca2+-triggered molecular switch. Cell 44:861-870.
Mostany R, Portera-Cailliau C (2008) A method for 2-photon imaging of blood flow in the neocortex through a cranial window. Journal of visualized experiments : JoVE.
Oray S, Majewska A, Sur M (2006) Effects of synaptic activity on dendritic spine motility of developing cortical layer v pyramidal neurons. Cereb Cortex 16:730-741.
Petreanu L, Mao T, Sternson SM, Svoboda K (2009) The subcellular organization of neocortical excitatory connections. Nature 457:1142-1145.
Ranson A, Cheetham CE, Fox K, Sengpiel F (2012) Homeostatic plasticity mechanisms are required for juvenile, but not adult, ocular dominance plasticity. Proc Natl Acad Sci U S A 109:1311-1316.
Rodriguez A, Ehlenberger DB, Dickstein DL, Hof PR, Wearne SL (2008) Automated three-dimensional detection and shape classification of dendritic spines from fluorescence microscopy images. PloS one 3:e1997.
Wallace H, Fox K (1999a) Local cortical interactions determine the form of cortical plasticity. J Neurobiol 41:58-63.
Wallace H, Fox K (1999b) The effect of vibrissa deprivation pattern on the form of plasticity induced in rat barrel cortex. Somatosens Mot Res 16:122-138.

Wallace H, Glazewski S, Liming K, Fox K (2001) The role of cortical activity in experience-dependent potentiation and depression of sensory responses in rat barrel cortex. J Neurosci 21:3881-3894.
White EL (1978) Identified neurons in mouse Sml cortex which are postsynaptic to thalamocortical axon terminals: a combined Golgi-electron microscopic and degeneration study. J Comp Neurol 181:627-661.
Wilbrecht L, Holtmaat A, Wright N, Fox K, Svoboda K (2010) Structural plasticity underlies experience-dependent functional plasticity of cortical circuits. J Neurosci 30:4927-4932.
Wright N, Glazewski S, Hardingham N, Phillips K, Pervolaraki E, Fox K (2008) Laminar analysis of the role of GluR1 in experience-dependent and synaptic depression in barrel cortex. Nat Neurosci 11:1140-1142.
Yang G, Pan F, Gan WB (2009) Stably maintained dendritic spines are associated with lifelong memories. Nature 462:920-924.
Yang G, Lai CS, Cichon J, Ma L, Li W, Gan WB (2014) Sleep promotes branch-specific formation of dendritic spines after learning. Science 344:1173-1178.
Yasumatsu N, Matsuzaki M, Miyazaki T, Noguchi J, Kasai H (2008) Principles of long-term dynamics of dendritic spines. J Neurosci 28:13592-13608.
Zuo Y, Yang G, Kwon E, Gan WB (2005) Long-term sensory deprivation prevents dendritic spine loss in primary somatosensory cortex. Nature 436:261-265.

Genotype	Deprivation	Rois	Mice	Initial Spines	Total Spines	Age range (days)	Baseline formation	Baseline elimination	Peak formation (deprived)	Peak elimination (deprived)
WT	Undeprived	15	5	478	715	70-125	3.78	3.53	-	-
WT	Chessboard	18	8	680	1501	75-107	4.22	4.35	17.87	11.66
WT	12 hour chessboard	4	1	88	180	63	3.86	3.42	31.58	25.72
WT	Chessboard (apical)	7	2	203	317	74-87	4.73	5.83	6.78	8.3
WT	All deprived	12	6	292	595	86-116	4.16	3.55	3.32	3.84
T286A	Undeprived	11	4	438	932	91-104	4.96	4.54	-	-
T286A	Chessboard	13	5	382	787	86-131	5.89	3.83	5.71	15.12

Table 1. Basic statistics for the different groups of animals studied. The number of Regions of interest (Rois), animals, original spines at the first observation point and total spines (new plus original) are given. The age range is for the start of the observation period and is in days postnatal. Baseline formation and baseline elimination rates are taken from the 2 or 3 baseline time points for the animals that will become deprived or across the entire observation period for undeprived cases. Formation and elimination values are expressed as percentages of the total number of spines present at the first time point and per day. All data for basal dendrites except where stated as apical.

	Filopodia	Stubby	Thin	Mushroom
Wild-type (all spines) undeprived	9	14	61	16
AP spines (day 1)	14	14	63	9
AP spines (day 14)	25	17	56	2
N spines (day 1)	26	35	31	8
NP spines (day 14)	28	13	54	5
CaMKII-T286A (all spines) undeprived	2	4	87	7

Table 2. Percentages of basal dendritic spines in different morphological classes by genotype and spine lifetime classification. AP = always persistent spines, either viewed 1 day after chessboard whisker deprivation or at 14. N = new spines produced on the first day of deprivation (day 1) and day 14. CamKII-T286A mice in the last row and wild-types in the first row were undeprived and the general population were classified independent of spine lifetime.

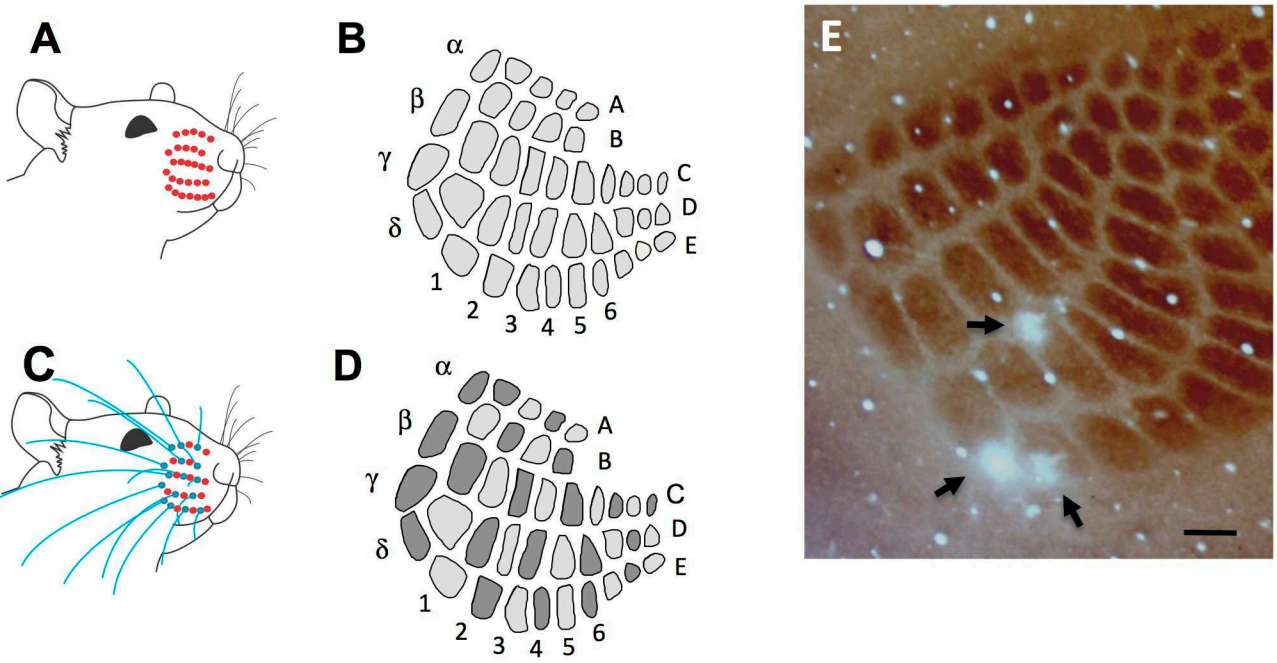
A
B
α
β
γ
δ
A
B
C
D
E
1
2
3
4
5
6
E
C
D
α
β
γ
δ
A
B
C
D
E
1
2
3
4
5
6

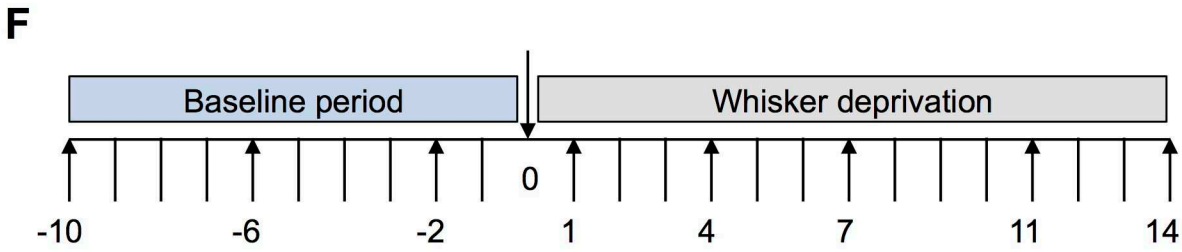
F
Baseline period
Whisker deprivation
0
-10
-6
-2
1
4
7
11
14

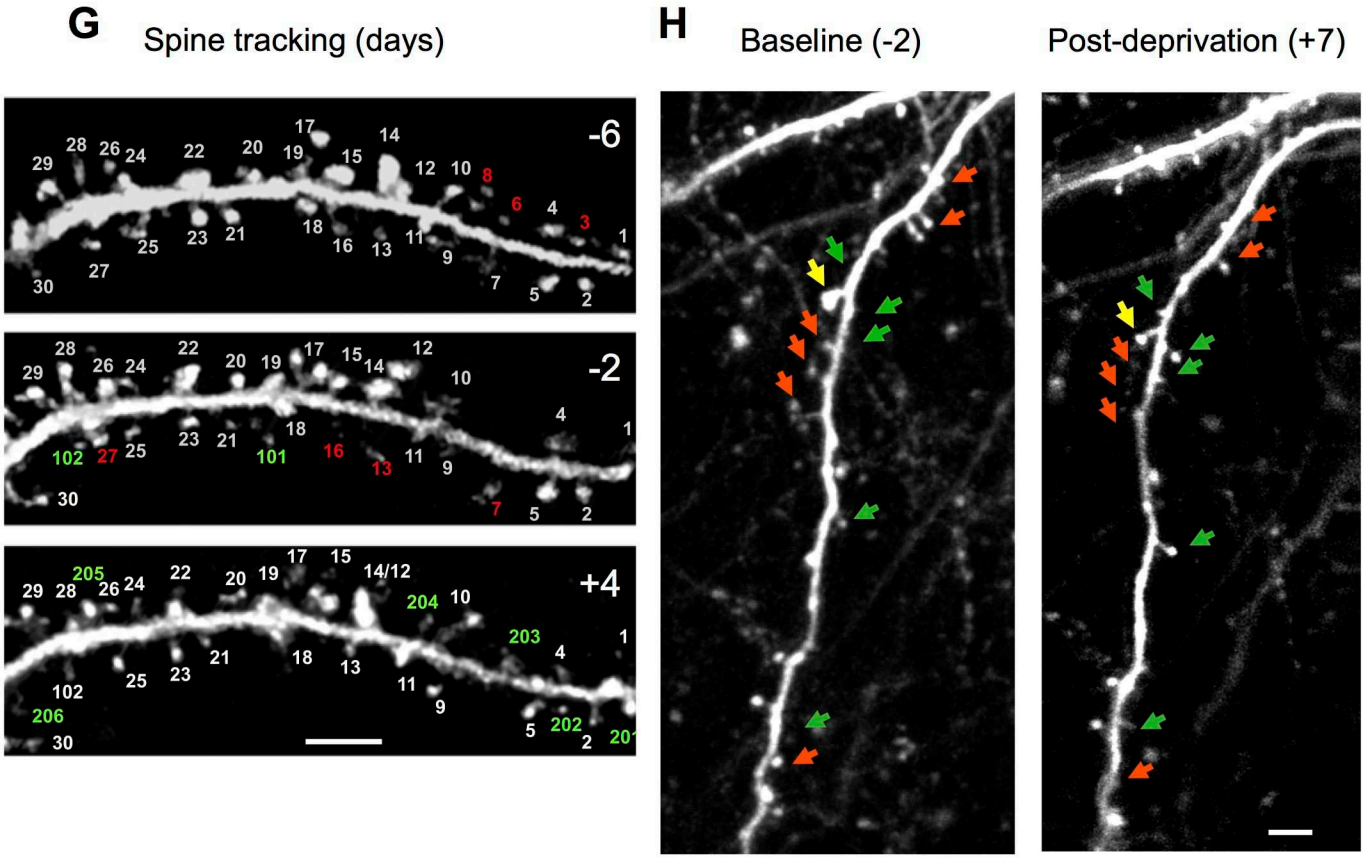
G
Spine tracking (days)
H
Baseline (-2)
Post-deprivation (+7)
-6
-2
+4

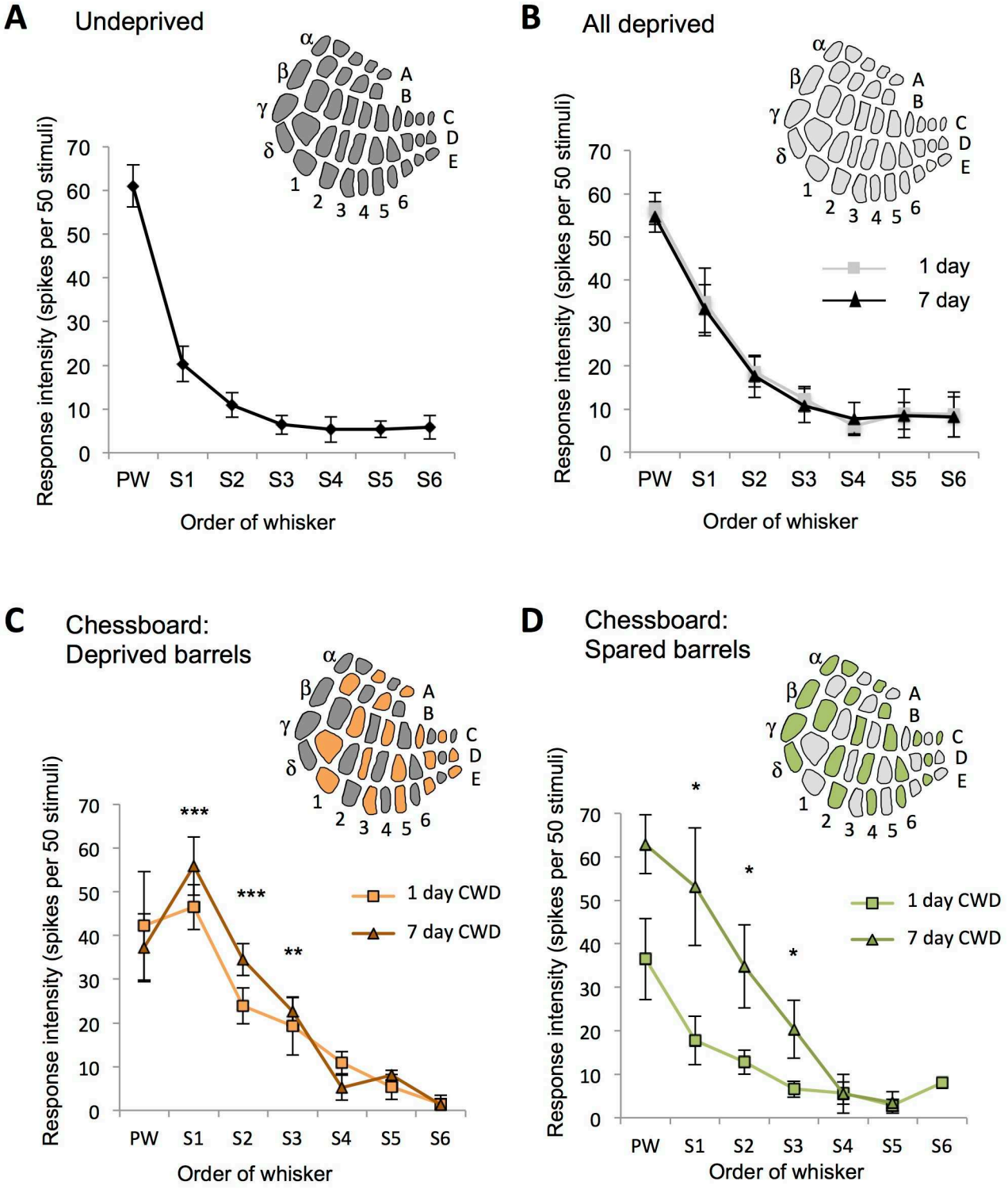
A
Undeprived
B
All deprived
C
Chessboard:
Deprived barrels
D
Chessboard:
Spared barrels
Response intensity (spikes per 50 stimuli)
Order of whisker
PW
S1
S2
S3
S4
S5
S6
1 day
7 day
1 day CWD
7 day CWD
α
β
γ
δ
A
B
C
D
E
1
2
3
4
5
6
***
**
*

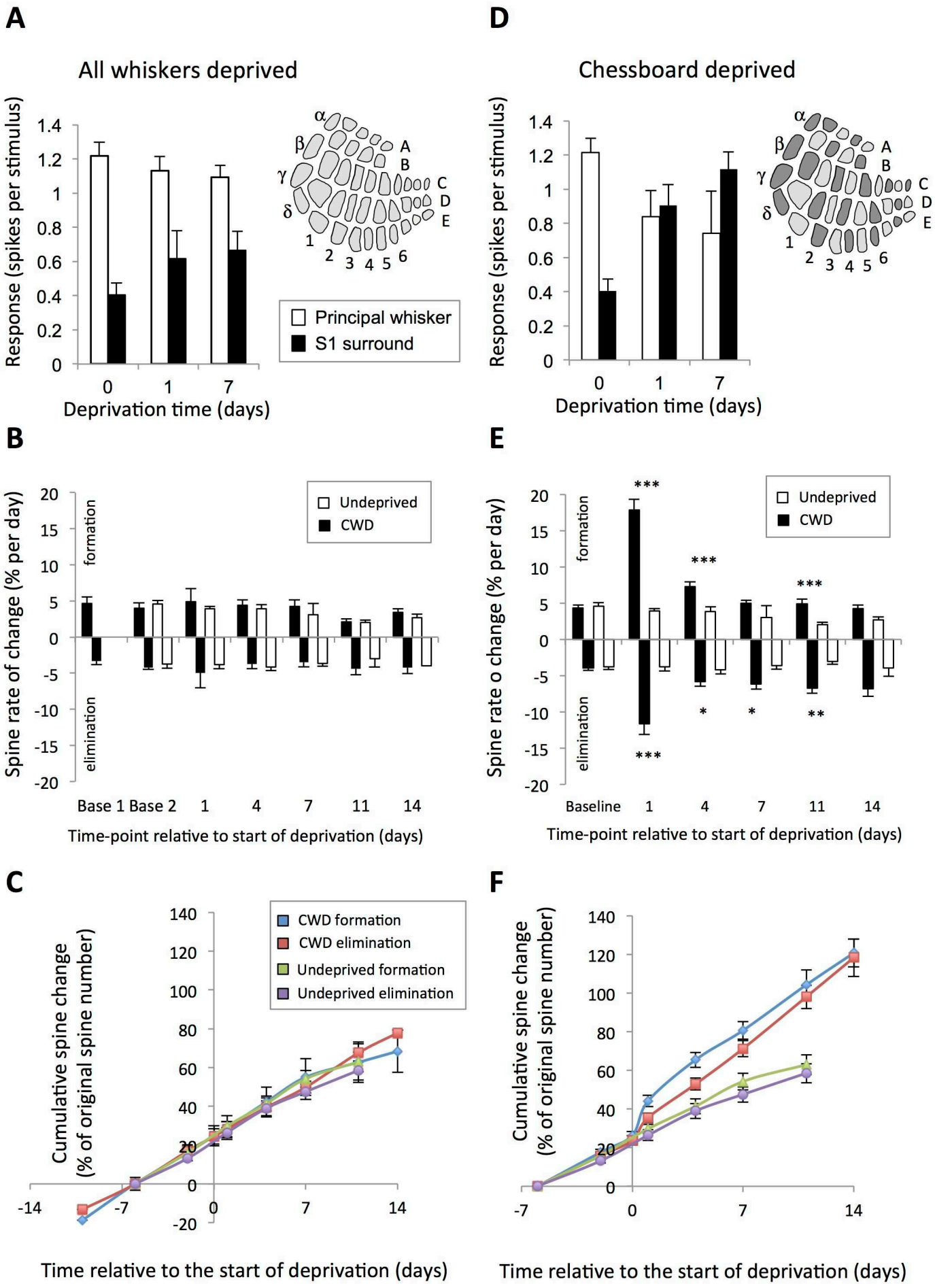
A
All whiskers deprived
Response (spikes per stimulus)
1.4
1.2
1
0.8
0.6
0.4
0.2
0
0
1
7
Deprivation time (days)
α
β
γ
δ
A
B
C
D
E
1
2
3
4
5
6
Principal whisker
S1 surround
D
Chessboard deprived
Response (spikes per stimulus)
Deprivation time (days)
B
Spine rate of change (% per day)
formation
elimination
Undeprived
CWD
Base 1
Base 2
1
4
7
11
14
Time-point relative to start of deprivation (days)
E
Spine rate o change (% per day)
***
*
**
Baseline
Time-point relative to start of deprivation (days)
C
Cumulative spine change (% of original spine number)
CWD formation
CWD elimination
Undeprived formation
Undeprived elimination
Time relative to the start of deprivation (days)
F
Cumulative spine change (% of original spine number)
Time relative to the start of deprivation (days)

Figure 4

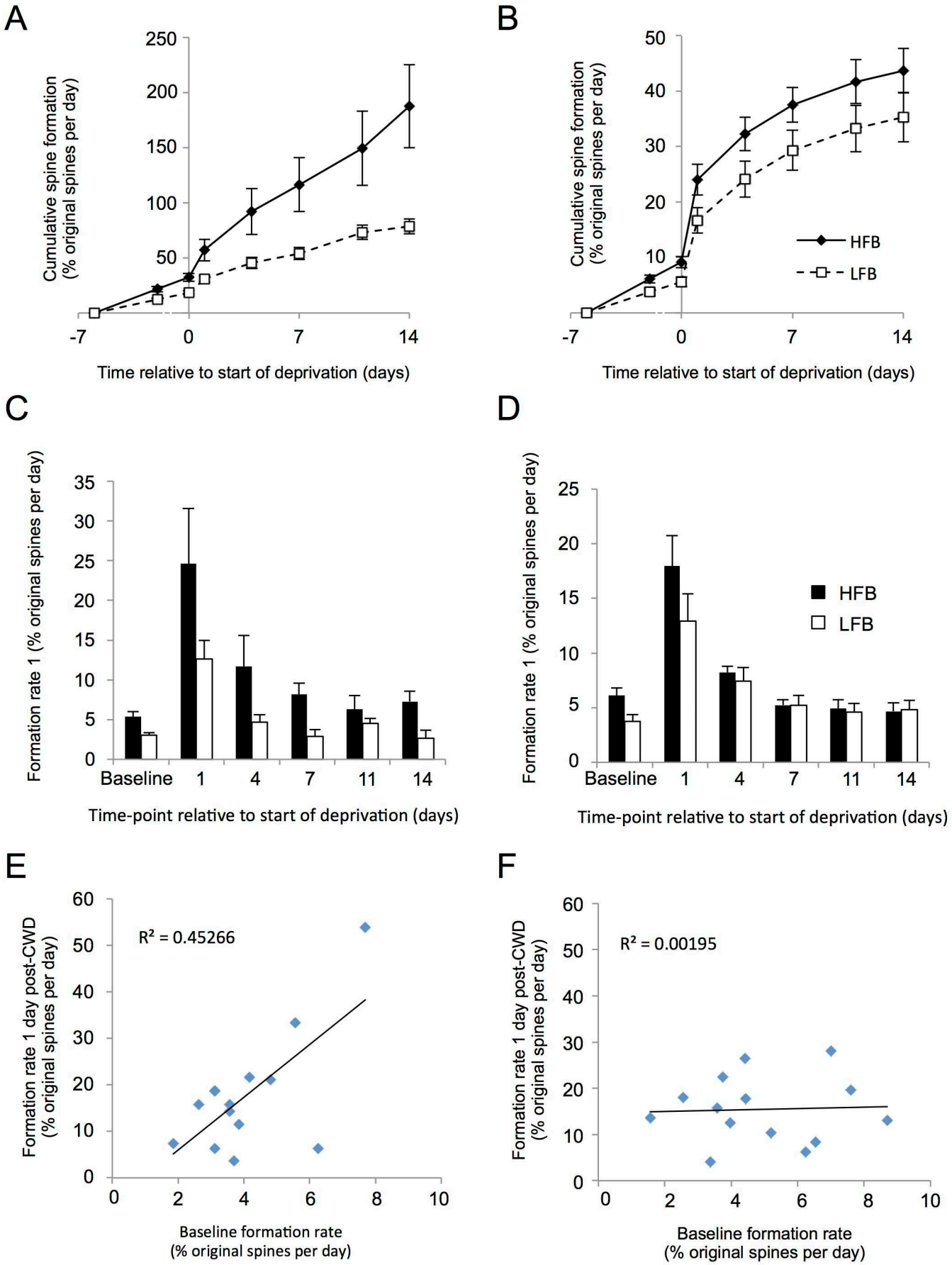
A
Cumulative spine formation (% original spines per day)
250
200
150
100
50
-7
0
7
14
Time relative to start of deprivation (days)
B
Cumulative spine formation (% original spines per day)
50
40
30
20
10
HFB
LFB
-7
0
7
14
Time relative to start of deprivation (days)
C
Formation rate 1 (% original spines per day)
35
30
25
20
15
10
5
0
Baseline
1
4
7
11
14
Time-point relative to start of deprivation (days)
D
Formation rate 1 (% original spines per day)
25
20
15
10
5
0
HFB
LFB
Baseline
1
4
7
11
14
Time-point relative to start of deprivation (days)
E
Formation rate 1 day post-CWD (% original spines per day)
R² = 0.45266
60
50
40
30
20
10
0
0
2
4
6
8
10
Baseline formation rate (% original spines per day)
F
Formation rate 1 day post-CWD (% original spines per day)
R² = 0.00195
60
50
40
30
20
10
0
0
2
4
6
8
10
Baseline formation rate (% original spines per day)

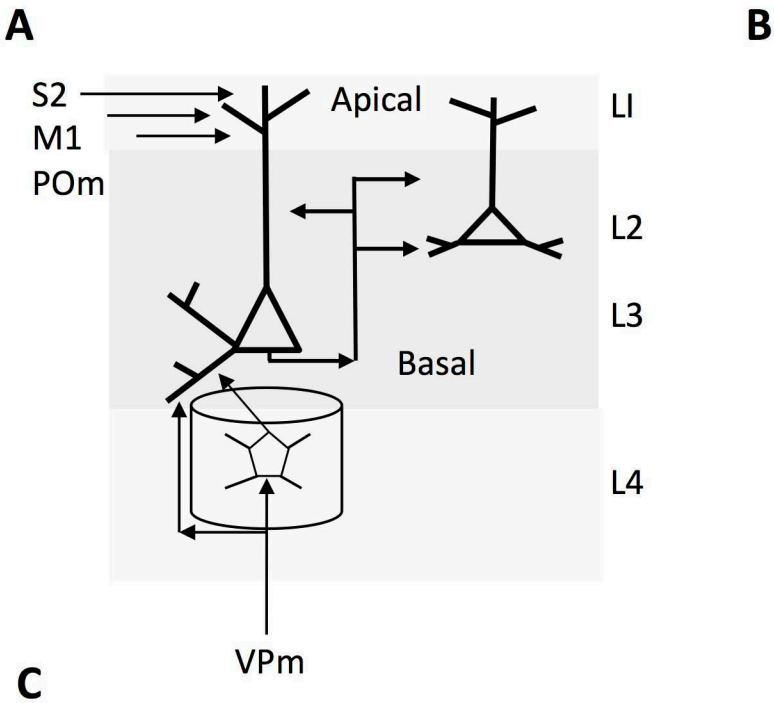
A
S2
M1
POm
Apical
LI
L2
L3
Basal
L4
VPm

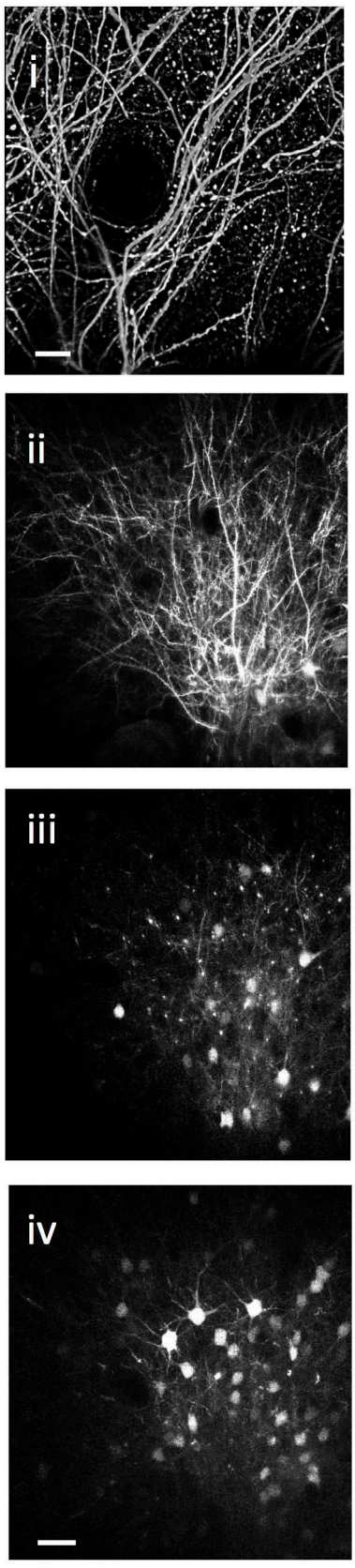
B
i
ii
iii
iv

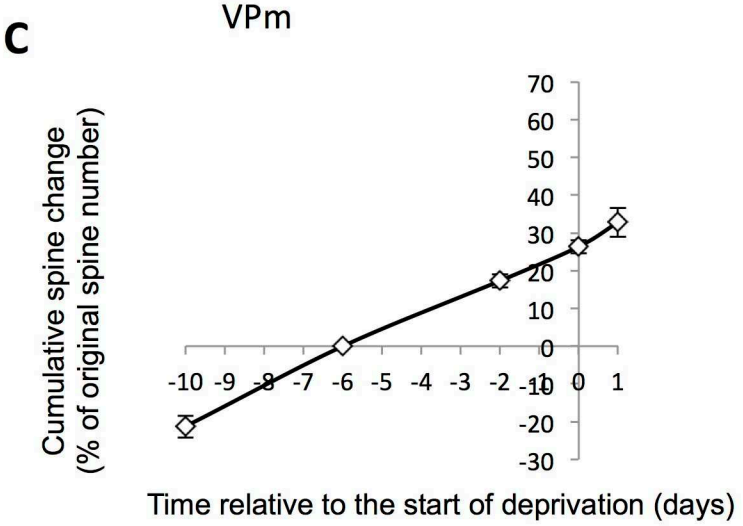
C
Cumulative spine change
(% of original spine number)
70
60
50
40
30
20
10
0
-10
-20
-30
-10 -9 -8 -7 -6 -5 -4 -3 -2 -1 0 1
Time relative to the start of deprivation (days)

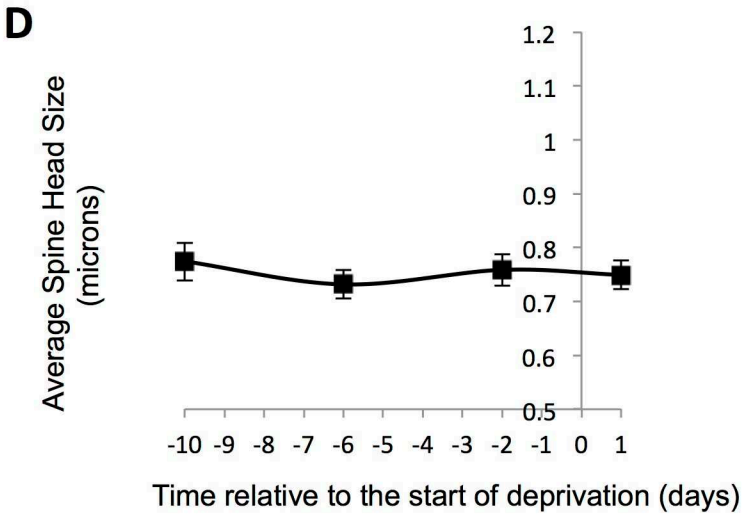
D
Average Spine Head Size
(microns)
1.2
1.1
1
0.9
0.8
0.7
0.6
0.5
-10 -9 -8 -7 -6 -5 -4 -3 -2 -1 0 1
Time relative to the start of deprivation (days)

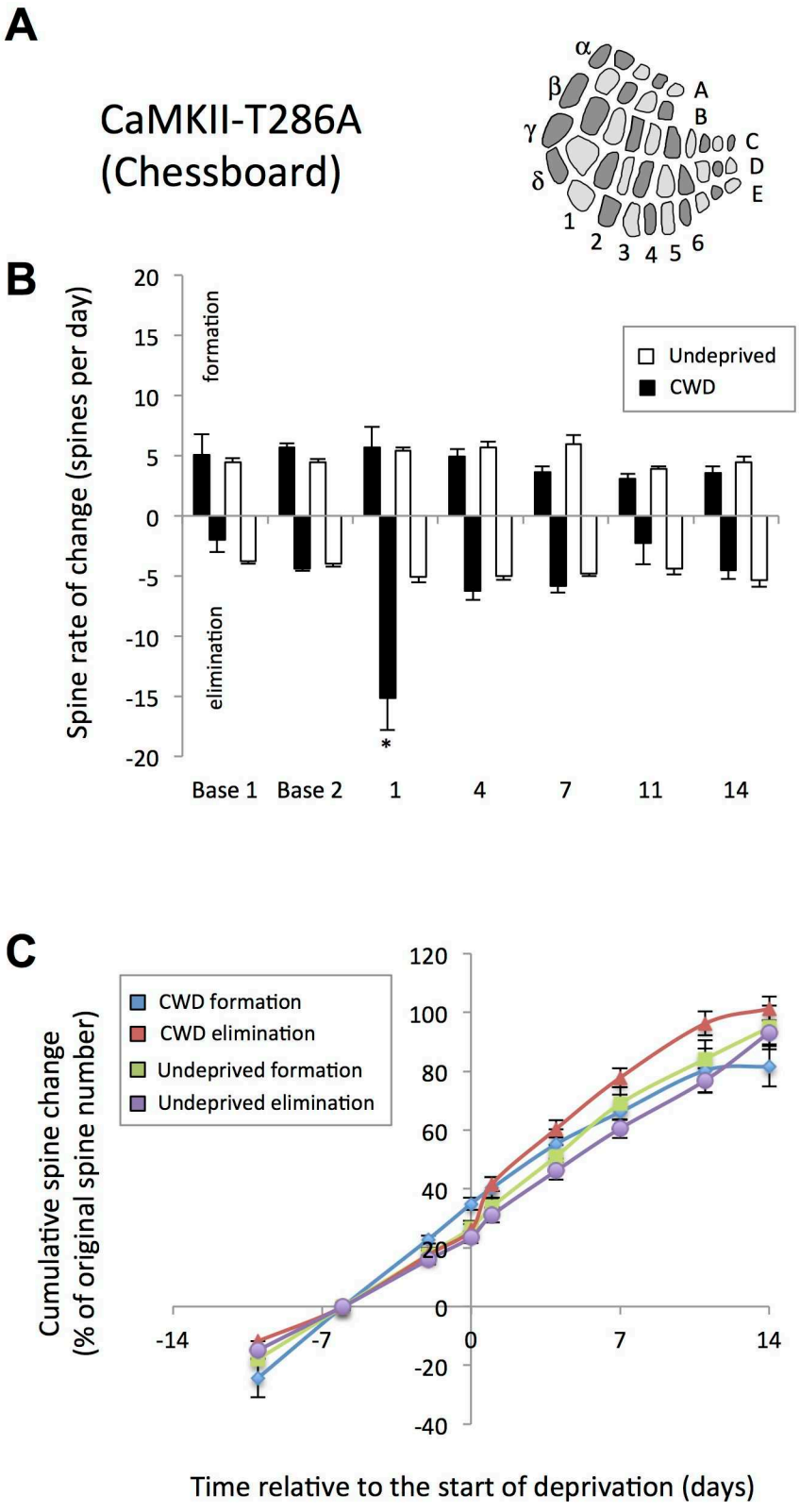
A
CaMKII-T286A
(Chessboard)
α
β
γ
δ
A
B
C
D
E
1
2
3
4
5
6
B
Spine rate of change (spines per day)
formation
elimination
Undeprived
CWD
20
15
10
5
0
-5
-10
-15
-20
*
Base 1
Base 2
1
4
7
11
14
C
Cumulative spine change
(% of original spine number)
CWD formation
CWD elimination
Undeprived formation
Undeprived elimination
120
100
80
60
40
20
0
-20
-40
-14
-7
0
7
14
Time relative to the start of deprivation (days)

Figure 7

A

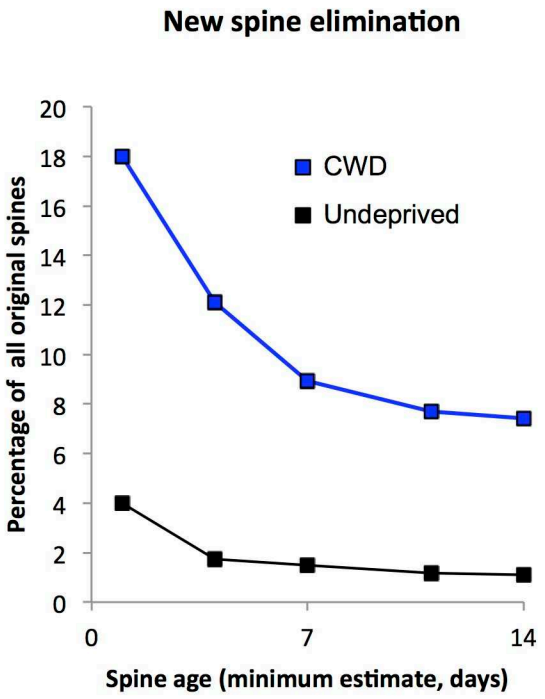
New spine elimination
Percentage of all original spines
20
18
16
14
12
10
8
6
4
2
0
0
7
14
Spine age (minimum estimate, days)
CWD
Undeprived

B

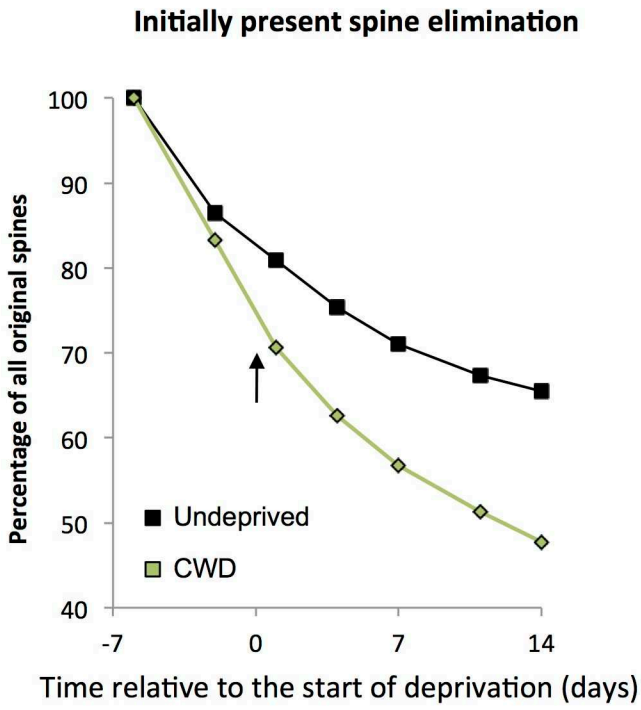
Initially present spine elimination
Percentage of all original spines
100
90
80
70
60
50
40
-7
0
7
14
Time relative to the start of deprivation (days)
Undeprived
CWD

Figure 8

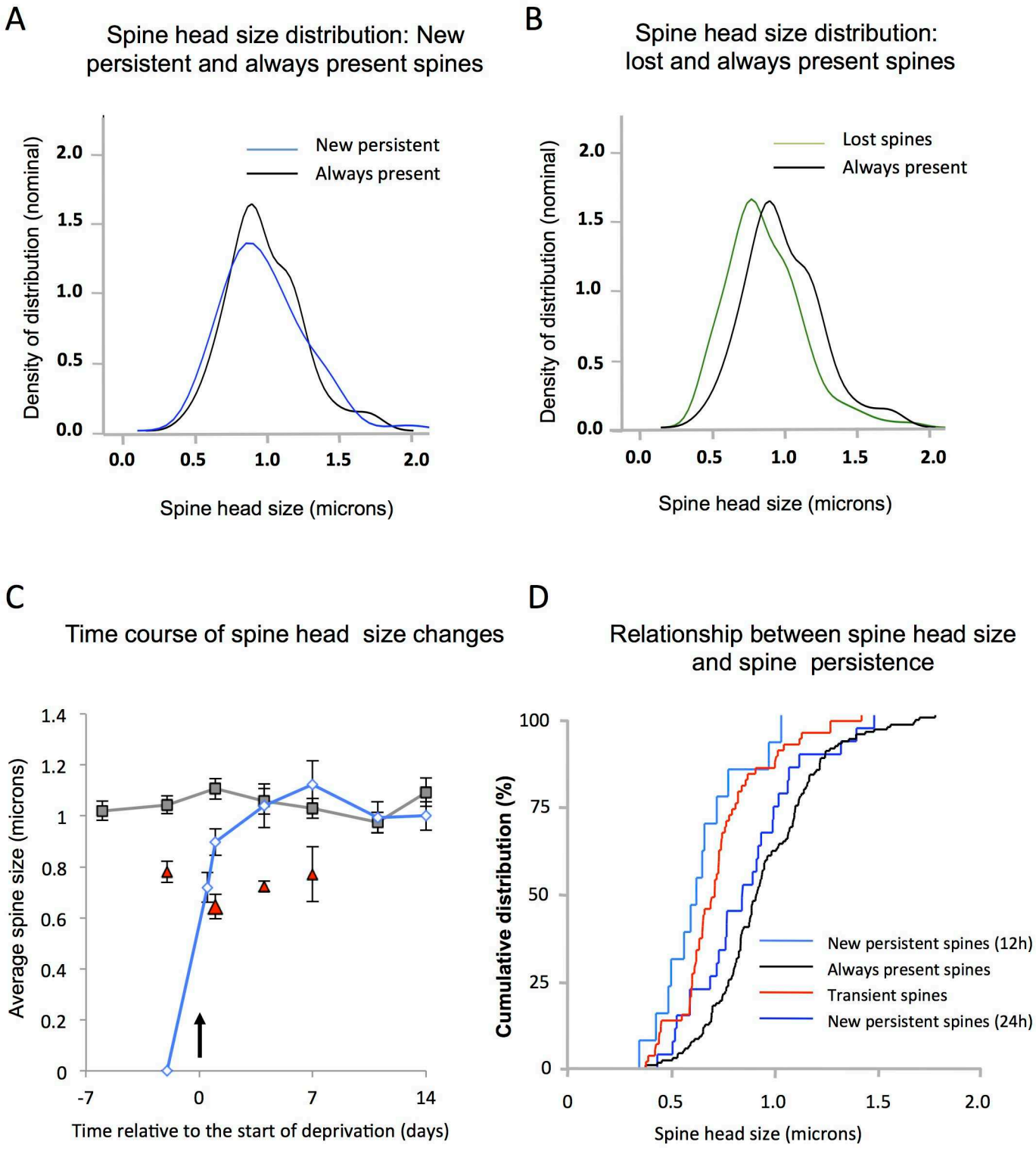
A
Spine head size distribution: New persistent and always present spines
New persistent
Always present
Density of distribution (nominal)
Spine head size (microns)
B
Spine head size distribution: lost and always present spines
Lost spines
Always present
Density of distribution (nominal)
Spine head size (microns)
C
Time course of spine head size changes
Average spine size (microns)
Time relative to the start of deprivation (days)
D
Relationship between spine head size and spine persistence
Cumulative distribution (%)
New persistent spines (12h)
Always present spines
Transient spines
New persistent spines (24h)
Spine head size (microns)

Figure 9

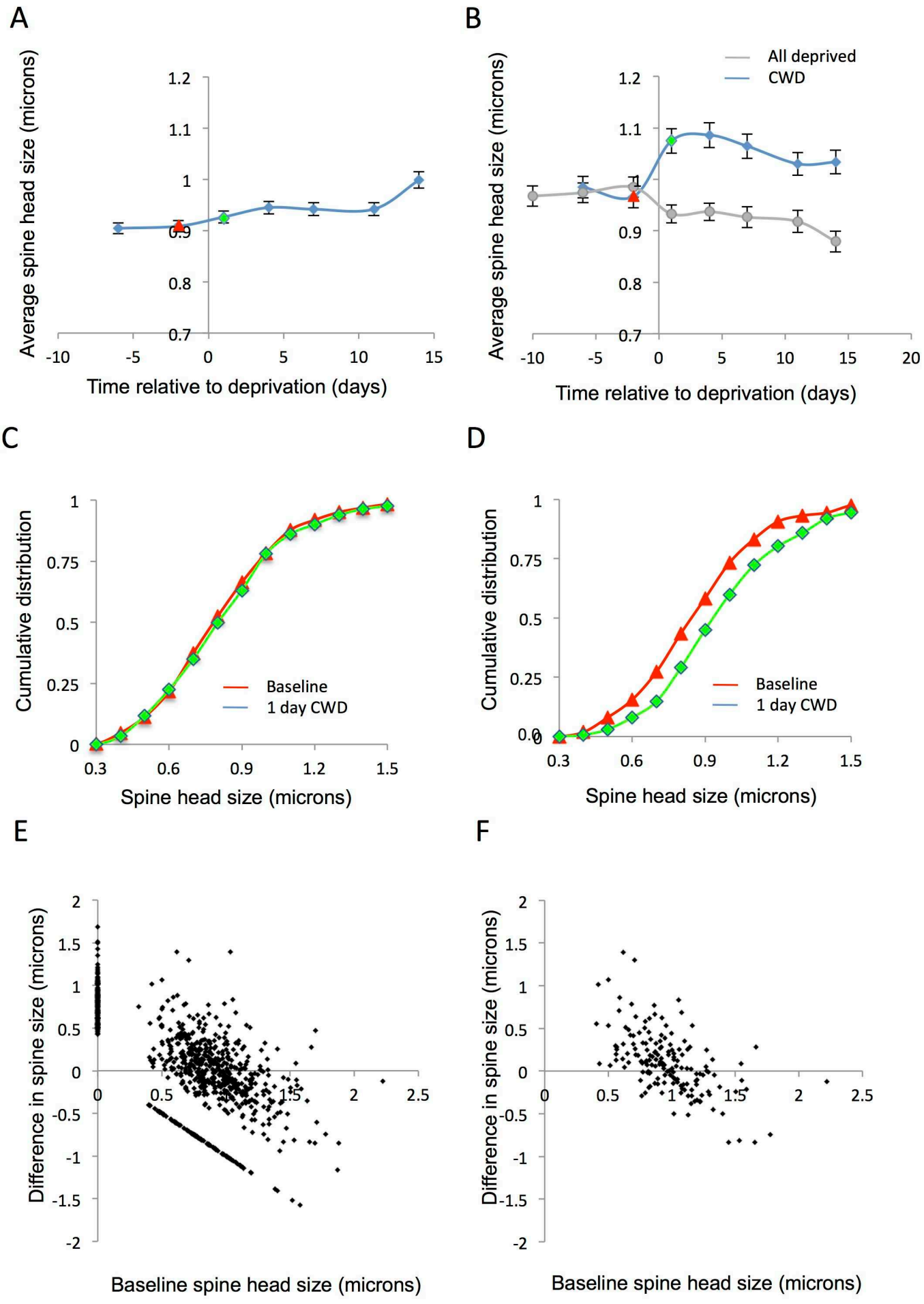
A
Average spine head size (microns)
1.2
1.1
1
0.9
0.8
0.7
-10
-5
0
5
10
15
Time relative to deprivation (days)
B
All deprived
CWD
Average spine head size (microns)
1.2
1.1
1
0.9
0.8
0.7
-10
-5
0
5
10
15
20
Time relative to deprivation (days)
C
Cumulative distribution
1
0.75
0.5
0.25
0
Baseline
1 day CWD
0.3
0.6
0.9
1.2
1.5
Spine head size (microns)
D
Cumulative distribution
1
0.75
0.5
0.25
0
Baseline
1 day CWD
0.3
0.6
0.9
1.2
1.5
Spine head size (microns)
E
Difference in spine size (microns)
2
1.5
1
0.5
0
-0.5
-1
-1.5
-2
0
0.5
1
1.5
2
2.5
Baseline spine head size (microns)
F
Difference in spine size (microns)
2
1.5
1
0.5
0
-0.5
-1
-1.5
-2
0
0.5
1
1.5
2
2.5
Baseline spine head size (microns)

Figure 10

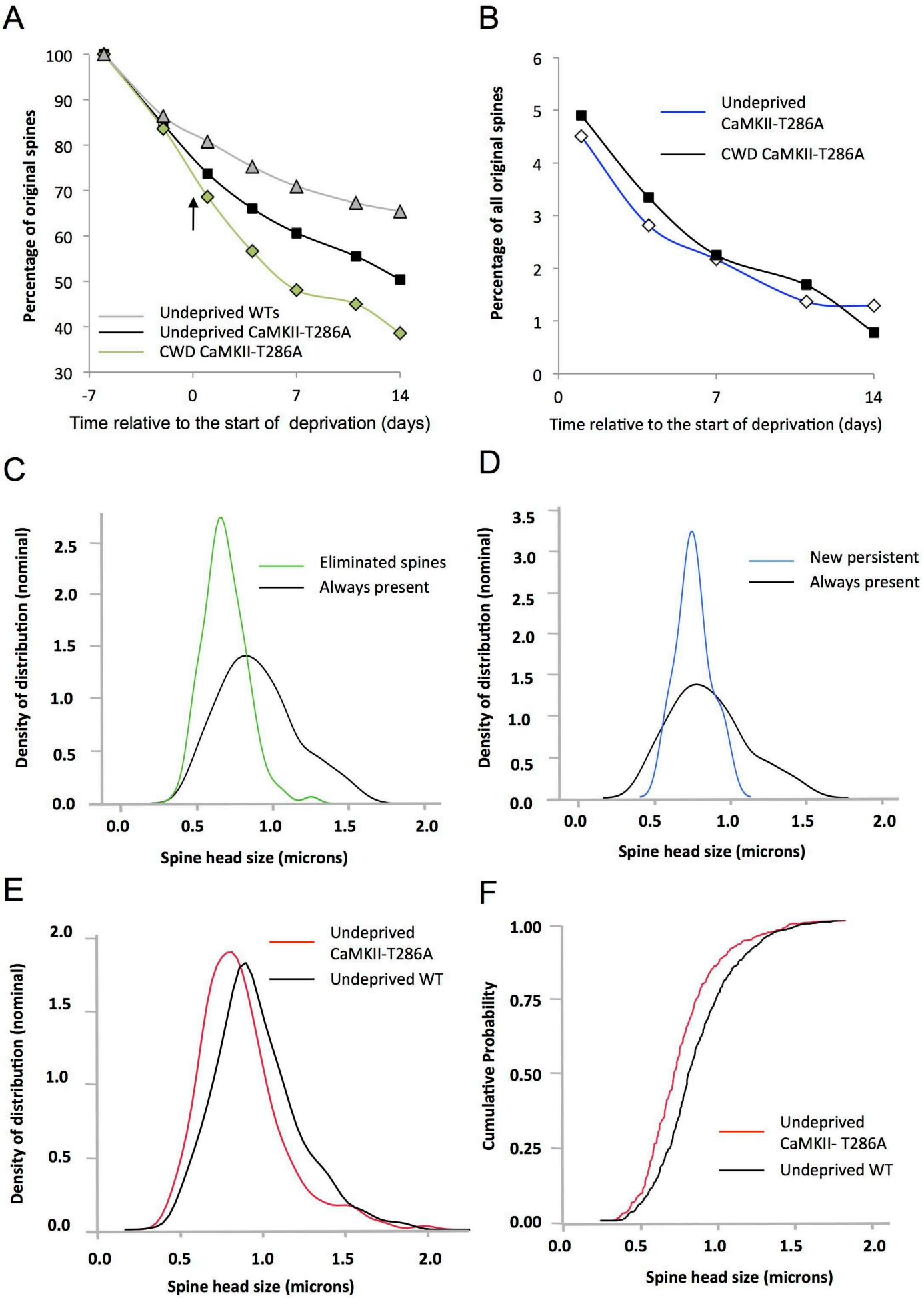
A
Percentage of original spines
100
90
80
70
60
50
40
30
-7
0
7
14
Time relative to the start of deprivation (days)
Undeprived WTs
Undeprived CaMKII-T286A
CWD CaMKII-T286A
B
Percentage of all original spines
6
5
4
3
2
1
0
0
7
14
Time relative to the start of deprivation (days)
Undeprived CaMKII-T286A
CWD CaMKII-T286A
C
Density of distribution (nominal)
2.5
2.0
1.5
1.0
0.5
0.0
0.0
0.5
1.0
1.5
2.0
Spine head size (microns)
Eliminated spines
Always present
D
Density of distribution (nominal)
3.5
3.0
2.5
2.0
1.5
1.0
0.5
0.0
0.0
0.5
1.0
1.5
2.0
Spine head size (microns)
New persistent
Always present
E
Density of distribution (nominal)
2.0
1.5
1.0
0.5
0.0
0.0
0.5
1.0
1.5
2.0
Spine head size (microns)
Undeprived CaMKII-T286A
Undeprived WT
F
Cumulative Probability
1.00
0.75
0.50
0.25
0.00
0.0
0.5
1.0
1.5
2.0
Spine head size (microns)
Undeprived CaMKII- T286A
Undeprived WT

Figure 11

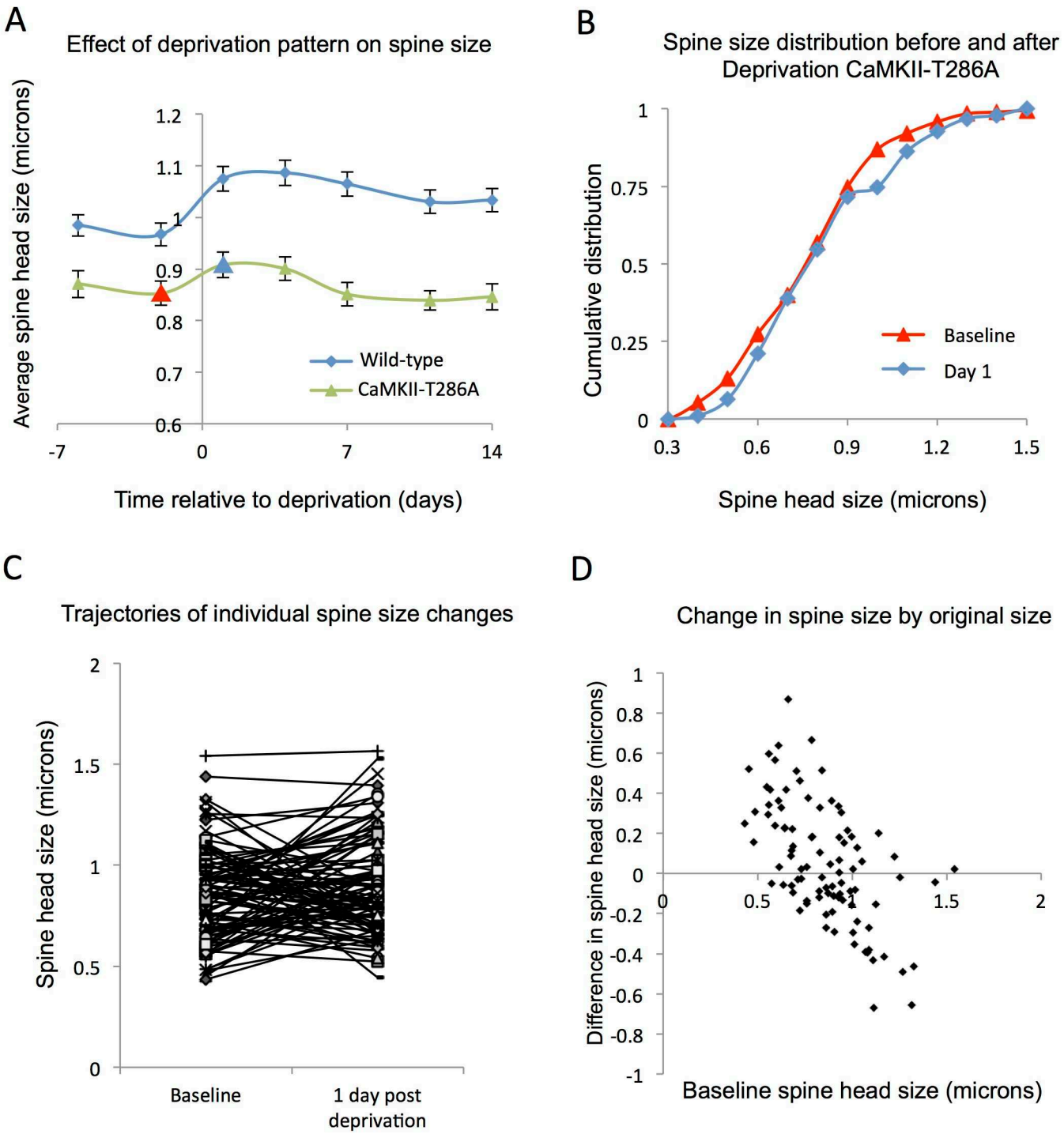
A
Effect of deprivation pattern on spine size
Average spine head size (microns)
1.2
1.1
1
0.9
0.8
0.7
0.6
-7
0
7
14
Wild-type
CaMKII-T286A
Time relative to deprivation (days)
B
Spine size distribution before and after Deprivation CaMKII-T286A
Cumulative distribution
1
0.75
0.5
0.25
0
0.3
0.6
0.9
1.2
1.5
Baseline
Day 1
Spine head size (microns)
C
Trajectories of individual spine size changes
Spine head size (microns)
2
1.5
1
0.5
0
Baseline
1 day post deprivation
D
Change in spine size by original size
Difference in spine head size (microns)
1
0.8
0.6
0.4
0.2
0
-0.2
-0.4
-0.6
-0.8
-1
0
0.5
1
1.5
2
Baseline spine head size (microns)